European Journal of Medicinal Chemistry 283 (2025) 117136

Contents lists available at ScienceDirect

European Journal of Medicinal Chemistry

journal homepage: www.elsevier.com/locate/ejmech

Research paper

Discovery of 22(*S*)-23-phenyl-24-norchol-5-en-3β,22-diol (PFM046) as the first-in-class, steroidal, non-sulfated Liver X Receptor antagonist with anticancer activity

Lorenzo Pontini [a,1], Tommaso Angelini [a,1], Pietro Palazzoli [a,1], Daniela Maggioni [b], Gianluca Giorgi [c], Laura Raccosta [b], Giuseppe Damiano [b], Valerio Mammoli [d], Niccolò Fontana [d], Vincenzo Russo [b,**], Maura Marinozzi [a,*]

[a] *Dipartimento di Scienze Farmaceutiche, Università degli Studi di Perugia, Via del Liceo, 1-06123, Perugia, Italy*
[b] *Immuno-Biotherapy of Melanoma and Solid Tumors Unit, Division of Experimental Oncology, IRCCS Scientific Institute San Raffaele, via Olgettina, 58-20132, Milan, Italy*
[c] *Department of Biotechnology, Chemistry and Pharmacy, University of Siena, Via A. Moro, 53100, Siena, Italy*
[d] *Center for Drug Discovery and Development-DMPK, Aptuit, an Evotec Company, Via A. Fleming 4, 37135, Verona, Italy*

ARTICLE INFO

Keywords:
Oxysterol derivatives
LXR antagonist
Anticancer agents
Semi-synthesis of steroids

ABSTRACT

A plethora of studies have demonstrated the crucial role played by Liver X Receptors (LXRs) in cancer. However, whether LXRs activation results in pro-*versus* anti-tumor effects is still matter of debate. Recently, we have reported the ability of 22(*S*)-hydroxycholesterol-3-sulfate (PFM037) to antagonize LXRα activity, and, at the same time, its capability to improve *in-vivo* anti-tumor immune responses. Herein we report the first study aimed at the definition of structure-activity relationships of PFM037. Successfully, we identified 22(*S*)-23-phenyl-24-norchol-5-en-3β,22-diol (PFM046) as a more potent LXRs antagonist than PFM037. PFM046 showed a peculiar LXR target gene expression profile, being able, as expected for an antagonist, to suppress SCD1 and FASN expression, while surprisingly maintaining the ability to upregulate ABCA1 gene, as typical for an agonist. PFM046 showed a remarkable antitumor activity in two both *in vitro*-and *in-vivo* mouse models, highlighting the high potential of LXRs antagonists in oncological applications.

1. Introduction

Oxysterols (OSs) are cholesterol's metabolites, structurally characterized by the presence of additional oxygenated functionalities other than the hydroxyl group at C-3 position already present in cholesterol. OSs play an important role in a plethora of physiological processes, including sterol transport, cholesterol homeostasis and innate immunity by modulating cell membrane fluidity and/or by binding with various proteins, including transporters, nuclear receptors, ion channels, and G-protein-coupled receptors [1].

A specific set of OSs, including 22(*R*)-hydroxycholesterol (22*R*–HC, **1**, Fig. 2), 24(*S*)-hydroxycholesterol (24*S*-HC, **2**), 25-hydroxycholesterol (25-HC, **3**), 5α,6α-epoxycholesterol (**4**), and 7-ketocholesterol (**5**) (Fig. 1) have been identified as the endogenous ligands of Liver X Receptors (LXRs) [2–4]. The levels of circulating OSs result from the net balance between their biosynthesis, catalysed by cytochrome P450 and non-eme iron-containing enzymes, and their catabolism, mainly undertaken by sulfotransferase 2B1b (SULT2B1b) [1,5]. SULT2B1b is a member of sulfotransferase family, highly expressed in human liver and macrophages, which operates the conversion of endogenous OSs into the corresponding 3-sulfates [5]. An intriguing point is the effect exerted by some endogenous oxysterol 3-sulfates on LXRs. In this respect, Song et al. [6] first demonstrated the ability of 5α,6α-epoxycholesterol-3-sulfate (**6**) and 7-ketocholesterol-3-sulfate (**7**) to function as LXRα antagonists (Fig. 1). Later on, 25-hydroxycholesterol-3-sulfate (25-HC3S, **8**) was identified as another endogenous LXR antagonist

* Corresponding author.
** Corresponding author.
E-mail addresses: russo.vincenzo@hsr.it (V. Russo), maura.marinozzi@unipg.it (M. Marinozzi).
[1] Present addresses: L. P., Procos SpA, Via G. Matteotti 249–28062 Cameri, (Italy); T. A., Chiesi Farmaceutici SpA, Via Palermo 26A - 43122 Parma, (Italy); P. P., Kemon SpA, Via E. Mattei 35 - San Giustino, (Italy).

https://doi.org/10.1016/j.ejmech.2024.117136
Received 26 July 2024; Received in revised form 2 December 2024; Accepted 2 December 2024
Available online 9 December 2024

able to inhibit SREBP-1 expression and activation with consequent decreases in ACC1, FASN, and HMGCR mRNA levels in hepatocytes and macrophages [7–9]. At the time 25HC3S (DUR-928, **8**) is in phase 2 clinical study for alcoholic hepatitis and in phase 1 clinical study for non-alcoholic steatohepatitis, and chronic kidney disease [10,11]. The biological profile of the sulfates **6**–**8** on LXRs proved to be opposite to that of their direct precursors, indicating that, in these cases, the sulfation does more than simply makes endogenous OSs easier eliminated. The diametrical ability of 25HC3S (**8**) and 25-HC (**3**) in regulating lipid metabolism and inflammatory response has been deeply investigated [9,12,13]. A parallel behaviour has been shown for 24*S*-HC (**2**) and the corresponding 3-and 24-monosulfates **9** and **10** (Fig. 2). The latter, indeed, were able to inhibit LXRα activation evoked by the agonist **2** in the FRET coactivator recruitment assay [14]. The biological profile of the exogenous C-22-epimer of **1**, namely 22(*S*)-hydroxycholesterol (22*S*-HC, **11**) is also worthy of mention (Fig. 2). In the seminal paper laying the groundwork for the structural requirements for LXR agonism, Janowski et al. [15] identified **11** as a high nanomolar competitive ligand of both LXR subtypes, but completely lacking efficacy. In 2001, Spencer et al. [16] described 22*S*-HC (**11**) as a functional antagonist based on LXRα LiSA and LXRα-GAL4 assays. However, it should be mentioned that this effect was observed when **11** was used at very high concentration (50–100 μM). Moreover, 22*S*-HC (**11**) was described as an LXR modulator able to abolish the upregulation of genes involved in fatty acid biosynthesis, in turn promoted by the non-steroidal LXRs agonist T0901317, without affecting other classical LXR target genes, such as ABCA1 and GLUT4 [17,18]. Thus, in the case of 22*R*–HC (**1**) the inversion of the configuration of C-22 proved to be the crucial event for the reversal of its biological activity on LXRs (see Fig. 2).

The marked effect on the biological profile towards LXRs played by the switching of the stereochemistry at C-22 does not restrict to the couple 22*R*–HC (**1**)/22*S*-HC (**11**); indeed, we observed a similar evidence in our in-house library of oxyphytosterols, too [19]: 22(*R*)-3β-stigmast-5-ene-3,22-diol (PFM014, **12**) was an efficacious agonist at both LXR isoforms, whereas the corresponding 22(*S*)-epimer **13** resulted completely inactive; the contrary occurred in the ergostane series where only 22(*S*)-3β-ergost-5,7-diene-3,22-diol (PFM003, **15**) was endowed with an agonistic profile (Fig. 2).

The role played by LXRs in cancer is still matter of debate: indeed, the answers to the question whether LXR activation may result in pro-*versus* anti-tumor effects are controversial [20]. The diverse expression of two LXRs isoforms by cancer cells as well by non-tumoral components of the tumor microenvironment and the different sensitivity of tumor-infiltrating immune cells to LXR activation/repression could explain the opposite results of different studies. Moreover, it should not be underestimated that the widespread usage of poor quality pharmacological probes may have led to misleading data [20]. In this scenario the paucity of available steroidal LXRs antagonist probes prompted us to synthesize sodium 22(*S*)-hydroxycholesterol-3-sulfate (PFM037, **16,** Fig. 3) assuming that the simultaneous presence of *S* absolute configuration at C-22 along with sulfate ester at C-3 would have provided a potent LXR antagonist. The ability of PFM037 (**16**) to antagonize LXRα activity in a dose-dependent manner with IC_{50} of 5.18 μM, along with its failure in activation of *ABCA1* transcript, while inhibiting *SREBP-1c*, *FASN* and *SCD1* mRNA proved the success of our design [21]. Even more interestingly PFM37 (**16**) was able to improve the anti-tumor immune response by increasing the number and differentiation of tumor-infiltrating Mono-DCs and/or by increasing the number of $CD3^+$

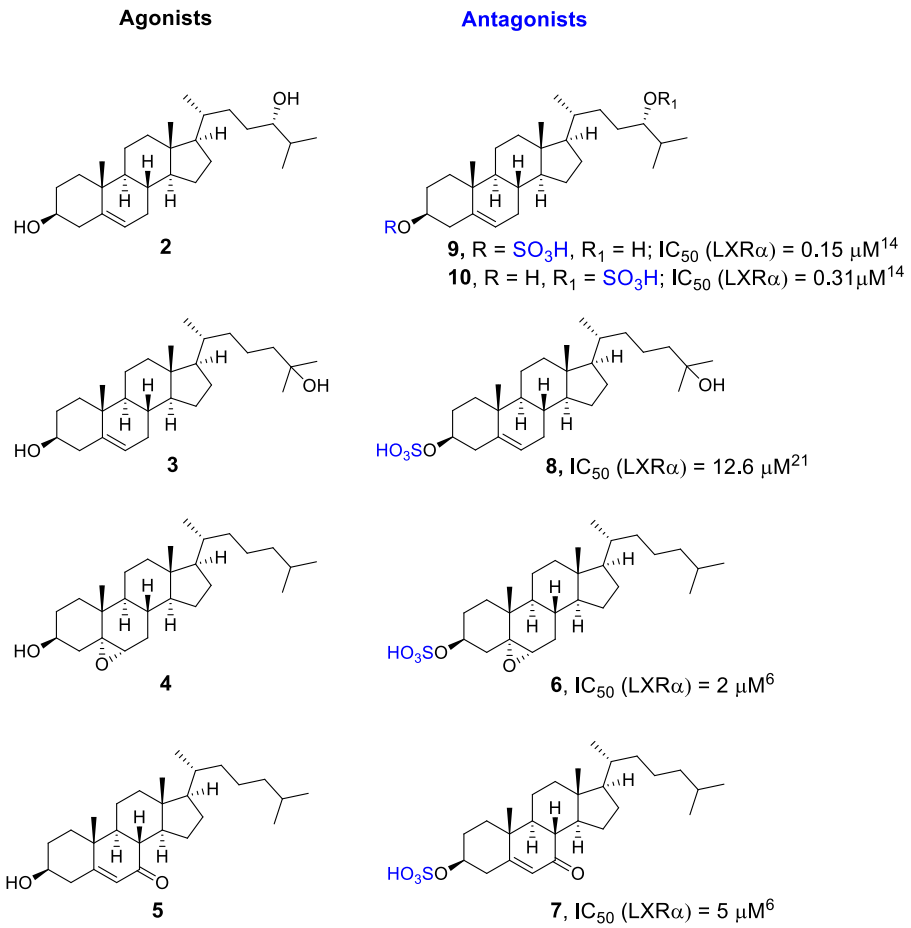

Fig. 1. From endogenous LXRs agonists (**2**–**5**) to endogenous LXRα antagonists (**7**-**10**): switching by sulfation.

and CD8$^+$ T-cells [21].

The identification of PFM037 (**16**) as the first-in-class steroidal LXR antagonist promoting anti-tumor immune responses prompted us to start a structure-activity relationship (SAR) study aimed to evaluate the influence of a) the presence of the sulfate ester, b) the stereochemistry at C-22, and c) the nature of side-chain's east-end. Among the first series of derivatives, including **17**, **18a-d** and **19a-d**, the successful and early identification of 22(*S*)-23-phenyl-24-norchol-5-en-3β,22-diol (PFM046, **18d**), as a potent LXR antagonist endowed with *in vitro* and *in vivo* antitumor properties, was the inspiration behind the design of the second series of derivatives **18e-j**, **20**–**25**, herein reported (Fig. 4).

2. Results and discussion

2.1. Chemistry and absolute configuration assignment

The key step for the preparation of all compounds was a Grignard addition of the suitable alkyl or aryl magnesium halide to 6β-methoxy-3α,5-cyclo-23,24-dinor-5α-cholan-22-al (**26**) [22] in the case of C-22-oxigenated derivatives (Scheme 1) or to 6β-methoxy-3α,5-cyclo-24-nor-5α-cholan-23-al (**27**, Schemes 5 and 6) for the C-23-oxigenated ones.

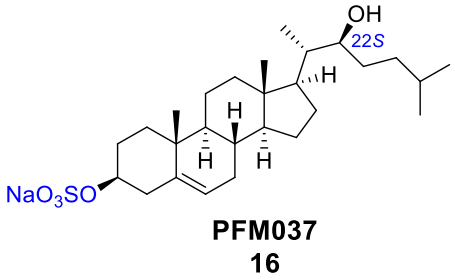

PFM037
16

Fig. 3. PFM037 (**16**) is a LXRα antagonist characterized by the presence of both C-22 (*S*) configuration and C-3 sulfate group.

As known, the Grignard addition performed on **26** proceeded with high stereoselectivity to afford, according to Cram's rule [23], almost exclusively the corresponding C-22 (*S*)-isomers **28a-k** with yields ranging from 50 to 76 %. The required organomagnesium reagent was either *in situ* generated or a commercial solution depending on the case (see experimental section for details). The recovery of 3β-hydroxy-5,6-ene moiety by acidic treatment gave the desired C-22(*S*)-hydroxyl derivatives **18a-j** starting from the corresponding **28a-j** (Scheme 1). The

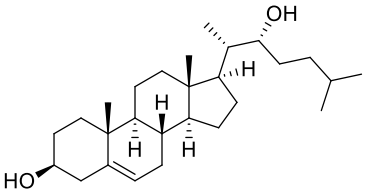

22*R*-HC
1
endogenous agonist

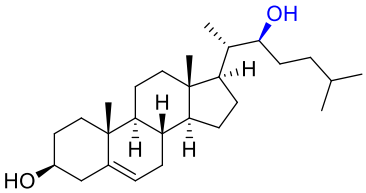

22*S*-HC
11
inactive
antagonist
negative modulator

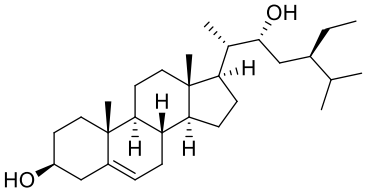

PFM014
12
potent agonist

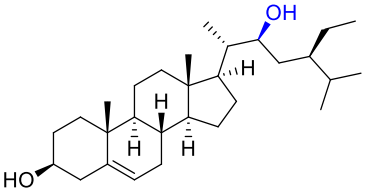

PFM012
13
inactive

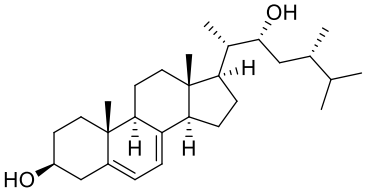

PFM004
14
inactive

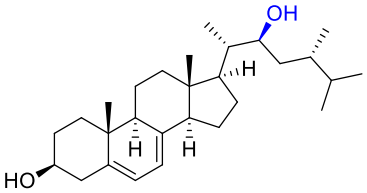

PFM003
15
agonist

Fig. 2. Modification of the biological profile of oxysterols on LXRs by inversion of the absolute configuration at C-22.

1^ series

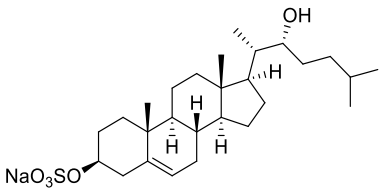

17

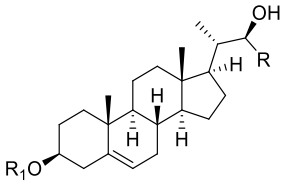

R = CH_3, R_1 = H, **18a**
R = CH_2CH_3, R_1 = H, **18b**
R = $CH_2CH(CH_3)_2$, R_1 = H, **18c**
R = $CH_2C_6H_5$, R_1 = H, **18d**
R = CH_3, R_1 = SO_3Na, **19a**
R = CH_2CH_3, R_1 = SO_3Na, **19b**
R = $CH_2CH(CH_3)_2$, R_1 = SO_3Na, **19c**
R = $CH_2C_6H_5$, R_1 = SO_3Na, **19d**

2^ series

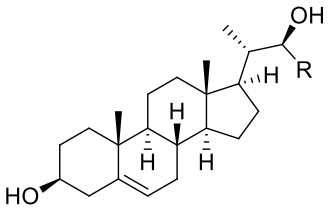

R = C_6H_5,,**18e**
R = $(CH_2)_2C_6H_5$,**18f**
R = $CH_2C_6H_{11}$,**18g**
R = CH_2(3-F-C_6H_4),**18h**
R = CH_2(4-F-C_6H_4),**18i**
R = CH_2(2-F-C_6H_4),**18j**

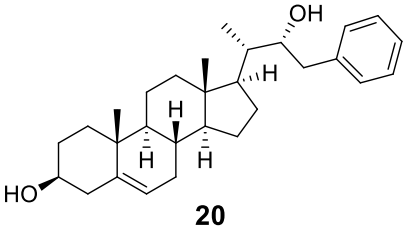

20

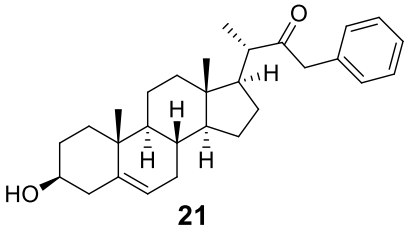

21

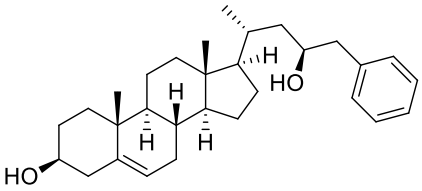

22

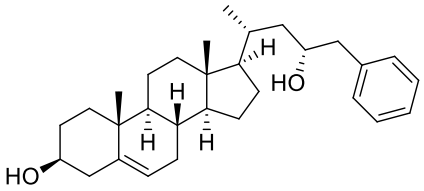

23

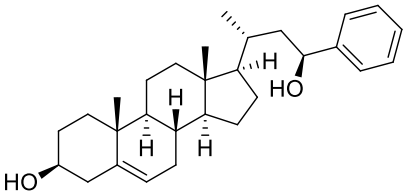

24

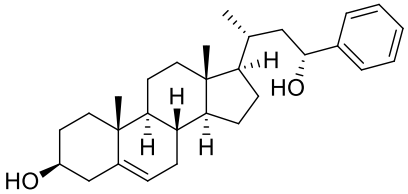

25

Fig. 4. Novel compounds described in this work.

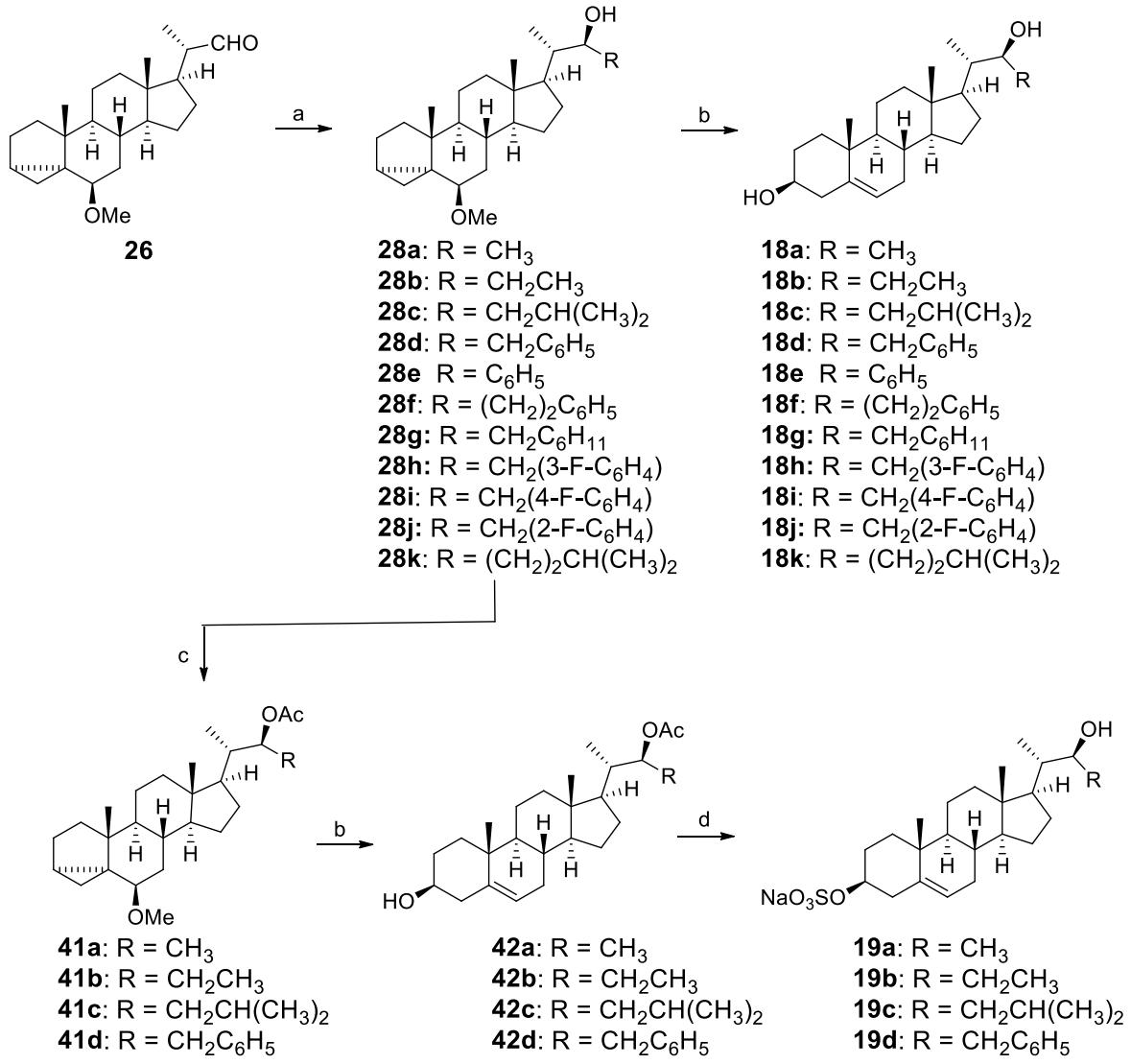

Scheme 1. Synthesis of 22(*S*)-hydroxy derivatives **18a-j**, and **19a-d**: (a) Grignard reagent, 0 °C to rt, 5–12 h; (b) *p*TsOH, dioxane/H_2O, 75 °C, 1–5 h; (c) Ac_2O, 4-DMAP, CH_2Cl_2, pyridine, rt, 14 h; (d) *i.* SO_3-pyridine complex, pyridine, rt, 4 h; *ii.* 1.25 M NaOH in MeOH, reflux for 1 h, then rt overnight.

inversion of the configuration of the hydroxyl group at C-22 was needed for the obtainment of compounds **17** and **20**. Thus, the intermediate **28k** was converted into the corresponding mesylate, in turn directly treated with potassium superoxide to obtain the desired C-22(*R*)-alcohol **29** in 70 % yield (Scheme 2). This protocol proved to be ineffective when applied to **28d**. On the contrary, cesium acetate successfully promoted the substitution of the intermediate mesylate in presence of 18-crown-6 in refluxing toluene to afford the desired C-22(*R*)-acetate **30** with full stereocontrol and with 34 % yield. The desired 22(*R*)-23-phenyl-24--norchol-5-en-3β,22-diol (**20**) was readily obtained from **30** after deacetylation in basic medium and further acidic restoration of the 3β-hydroxy-5,6-ene moiety with 70 % overall yield (Scheme 3).

The preparation of the corresponding 22-keto derivative **21** was performed by Dess-Martin oxidation of **28d** to get **31**, in turn submitted to the final acidic restoration of the A/B rings system (Scheme 3). As mentioned above the preparation of the C-23-hydroxy derivatives **22**–**25** required as starting material 6β-methoxy-3α,5-cyclo-24-nor-5α-cholan-23-al (**27**), whose synthesis was firstly reported by Djerassi and coll. starting from **26** (Scheme 4) [24]. In particular, the Authors exploited *n*-BuLi as the base required for the phosphorus ylide formation in the one-carbon homologation step of **26**. In our hands this protocol did not work efficiently and then different reaction conditions were screened. To our delight, by changing the reaction solvent from ether to toluene and the base into potassium *tert*-pentoxide the alkene **32** was obtained in 97 % yield.

With **32** in hands, the aldehyde **27** was readily available after a completely regioselective hydroboration/oxidation reaction and subsequent pyridinium chlorocromate (PCC) oxidation of the resulting primary alcohol **33**, thus obtained (Scheme 4). Grignard reaction with benzylmagnesium bromide gave the almost equimolar mixture of the two C-23-hydroxy epimers **34** and **35** starting from **27** (Scheme 5). A careful medium pressure chromatography (mpc) made possible the obtainment of the single pure diastereoisomers **34** and **35** in 51 % overall yield. Each epimer was then converted into the corresponding desired compounds **22** and **23**, respectively, by A/B rings system restoration in acidic conditions (Scheme 5).

Analogously, the treatment of **27** with phenylmagnesium bromide afforded the mixture of the two C-23-phenyl derivatives **36** and **37**, inseparable to this stage. The separation by mpc was instead possible after transforming the two components into the corresponding 3β-acetates **38** and **39** by treatment with glacial acetic acid. Further transesterification of **38** in the presence of potassium carbonate gave the desired 23(*S*)-23-phenyl-24-norchol-5-en-3β,23-diol (**24**). By an analogous procedure the corresponding C-23(*R*)-epimer **25** was obtained

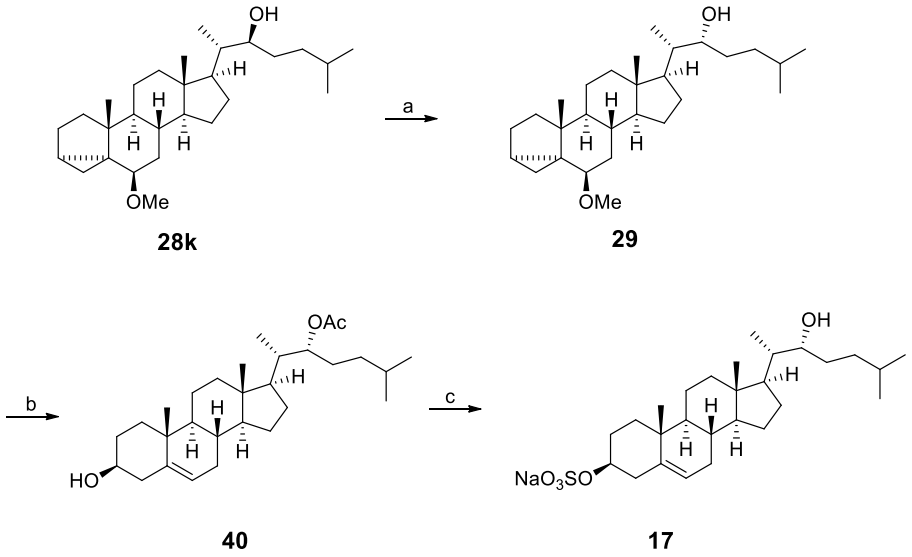

Scheme 2. Synthesis of sodium 22(*R*)-hydroxycholesterol 3-sulfate (**17**): (a) *i.* CH_3SO_2Cl, CH_2Cl_2, pyridine, rt, 20 h. *ii.* KO_2, DMSO, DMF, 18-crown-6, rt, 24 h; (b) *i.* Ac_2O, 4-DMAP, CH_2Cl_2, pyridine, rt, 14 h; *ii.* *p*TsOH, dioxane/H_2O, 75 °C, 1 h; (c) *i.* SO_3-pyridine complex, pyridine, rt, 4 h; *ii.* 1.25 M NaOH in MeOH, reflux for 1 h, then rt overnight.

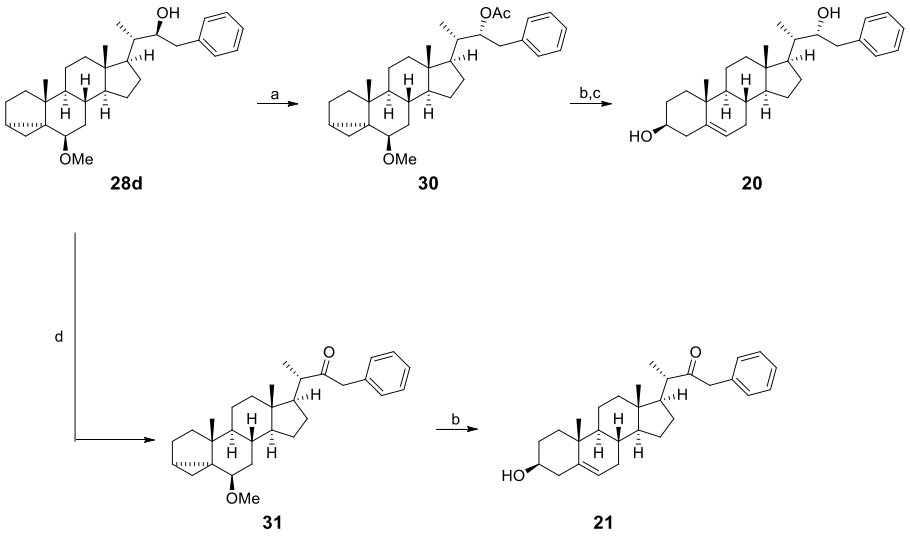

Scheme 3. Synthesis of 22(*R*)-23-phenyl-24-norchol-5-en-3β,22-diol (**20**) and 3β-hydroxy-23-phenyl-24-norchol-5-en-22-one (**21**): (a) *i.* CH_3SO_2Cl, pyridine, rt, 15 h. *ii.* CsOAc, 18-crown-6, toluene, reflux, 24 h; (b) *p*TsOH, dioxane/H2O, 75 °C, 2.5 h; (c) $NaOH_{aq}$, MeOH, reflux, 1 h; (d) Dess-Martin reagent, CH_2Cl_2, rt, 3 h.

starting from **39** (Scheme 6).

The almost complete lack in the literature of C-23-hydroxysterol analogous to our compounds **22**–**25** kept us from attributing the absolute configuration of the newly created chiral centres on the basis of the relatively small differences observed in the NMR spectra of both couples of epimers, namely **22** *versus* **23** and **24** *versus* **25**. Therefore, to unambiguously assign the absolute configuration at C-23 the derivatives **22** and **25** were submitted to single crystal X-ray analysis (Fig. 5A and B,

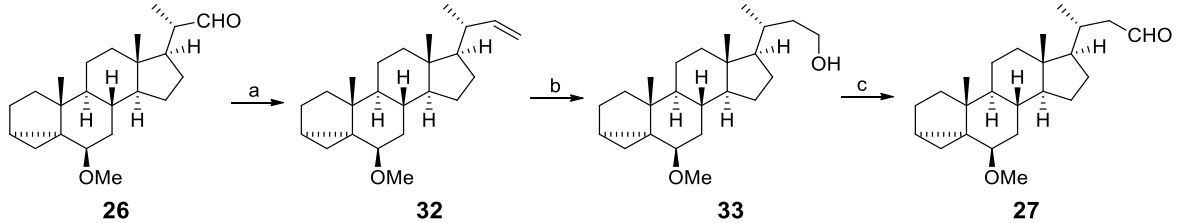

Scheme 4. Synthesis of 6β-methoxy-3α,5-cyclo-24-nor-5α-cholan-23-al (**34**): (a) CH_3PPh_3Br, 1.7 M potassium *tert*-pentoxide in toluene, toluene, rt to 70 °C, 1 h; (b) *i.* 1 M BH_3•THF, THF, 0 °C, 2.5 h; *ii.* H_2O_2, $NaOH_{aq}$, 0 °C, to rt, 1 h; (c) PCC, CH_2Cl_2, 1 h.

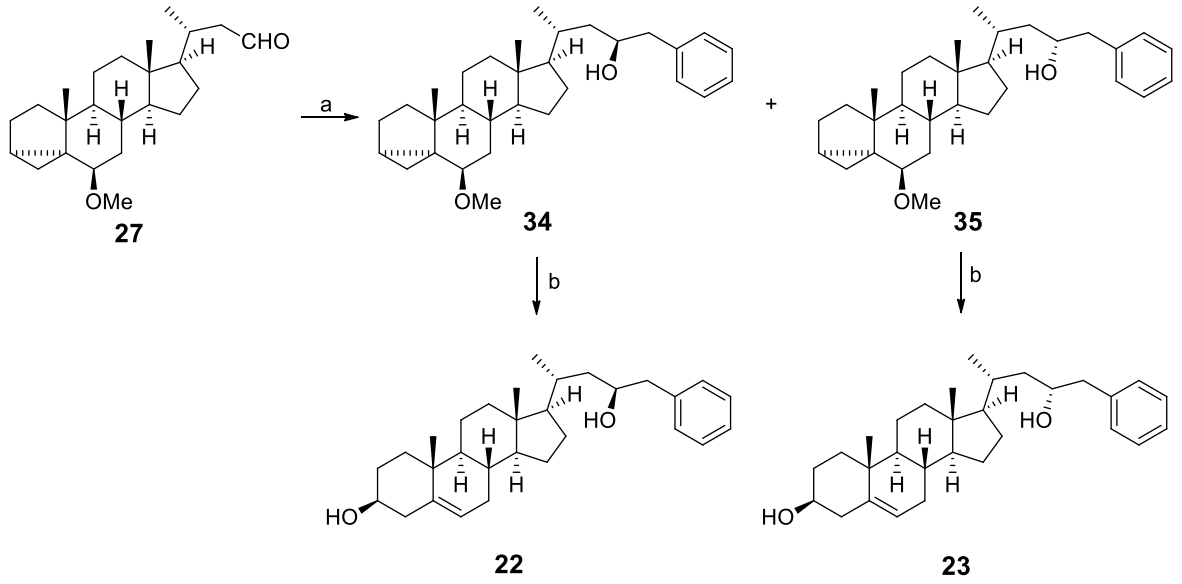

Scheme 5. Synthesis of 23(*S*)- and 23(*R*)-24-phenylchol-5-en-3β,23-diols (**22** and **23**): (a) *i.* $C_6H_5CH_2MgBr$, THF, 0 °C to rt, 15 h; *ii.* mpc; (b) *p*TsOH, dioxane/H_2O, 75 °C, 1 h.

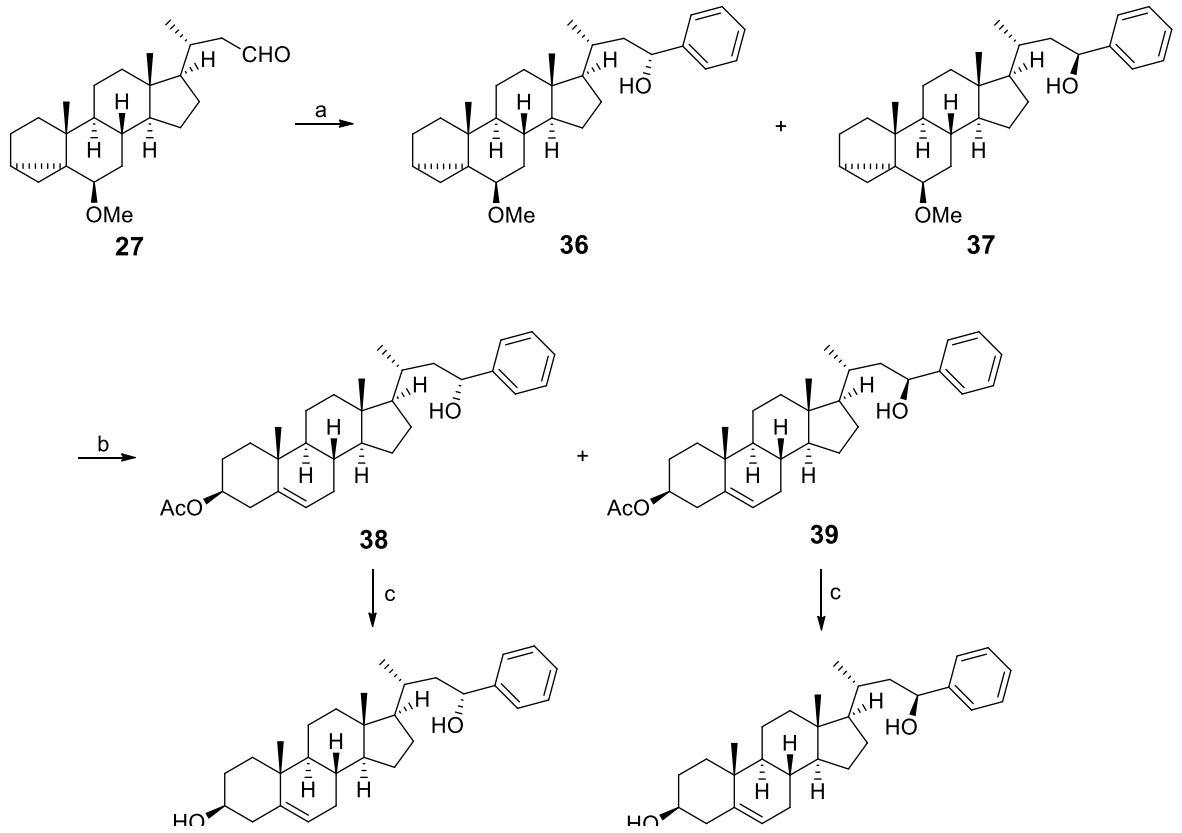

Scheme 6. Synthesis of 23(*S*)- and 23(*R*)-23-phenyl-24-norchol-5-en-3β,23-diols (**24** and **25**): (a) *i.* C_6H_5MgBr, THF, 0 °C to rt, 15 h; (b) *i.* glacial AcOH, 75 °C, 2.5 h; *ii.* mpc; (c) K_2CO_3, THF/MeOH, rt, 6 h.

respectively). Thus, they were definitively characterized as 23(*S*)-24-phenylchol-5-en-3β,23-diol (**22**) and 23(*S*)-23-phenyl-24-norchol-5-en-3β,23-diol (**25**).

The desired C-3-sulfates **17** and **19a-d** were all synthesized starting from the parent 22-hydroxy-3α,5α-cyclo-6β-methoxy derivatives **28k** and **28a-d**, respectively**,** by a general three steps route designed to selectively provide sulfation at C-3, namely: 1) protection of the side-chain hydroxyl group as acetate; 2) acidic *i*-ether hydrolysis and 3) sulfation reaction, followed by alkaline treatment (Schemes 1 and 2). Acetylation reaction of **29** furnished the corresponding 22(*R*)-acetate

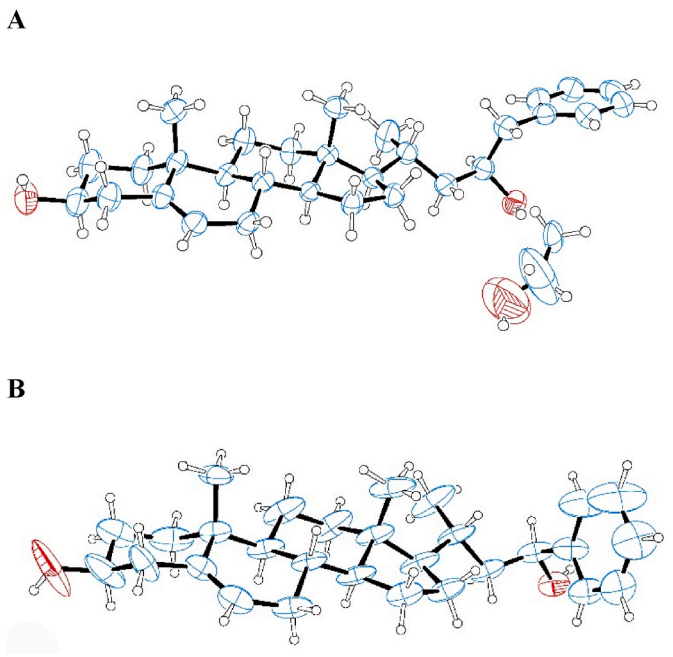

Fig. 5. A, Crystal structure of compound **22** with a crystallization ethanol molecule; B, Crystal structure of compound **25**. A crystallization water molecule is omitted for clarity. Ellipsoids enclose 50 % probability.

directly treated with *p*-toluenesulfonic acid in aqueous dioxane to give the desired 3β-hydroxy-22-acetoxy derivative **40** in 70 % overall yield (Scheme 2). The conversion of the latter into the title sulfate derivative **17** was realized by a modification of a reported method [25], involving the treatment of **40** with sulfur trioxide pyridine complex at room temperature, the recovery by filtration of the obtained 22-acetoxy-3-sulfate, finally treated with methanolic sodium hydroxide solution. At the end of the reaction the addition of water promoted the precipitation of the pure desired 22(*R*)-hydroxycholesterol-3-sulfate sodium salt (**17**, Scheme 2). By an analogous synthetic protocol, the C-3-sulfates **19a-d** were obtained starting from **28a-d** (Scheme 1).

2.2. *In-vitro Pharmacology and SAR considerations*

Our first aim was to verify if the sulfation of the hydroxyl group at C-3 of the endogenous agonist 22*R*–HC (**1**) would have caused the switching of its biological profile from LXRs agonist to antagonist. That's because the synthesis and the biological evaluation of sodium 22(*R*)-hydroxycholesterol-3-sulfate (**17**) had not been yet reported. Once prepared, the ability of **17** to activate LXRs was assessed by using luciferase assays with GAL-4 chimeric receptors. These were performed by co-transfecting plasmids encoding *h*LXR-α and-β binding domains fused to GAL-4, with the respective responsive element conjugated with the luciferase reporter gene into the human embryonic kidney 293 cells.

At the concentration of 10 μM **17** resulted unable to activate both LXRα (Fig. 6A) and LXRβ (Fig. 6B), thus proving that the sulfation at C-3, as expected, abolished the ability of the parent oxysterol **1** to act as LXR agonist. Then, **17** was evaluated in a competition assay *versus* the endogenous agonist **1** to assess its potential antagonist profile. Again, **17** was unable to reduce 22*R*–HC (**1**)-promoted activation on both isoforms (Fig. 7), leading us to conclude that the only presence of the sulfate at C-3 was not enough to ensure the switching from agonist to antagonist in the case of 22*R*–HC (**1**), differently from what reported for the other endogenous agonists **2**, **3** and **5**.

Thus, once becoming aware of the central role of the *S* absolute configuration at C-22 in determining the antagonism of PFM037 (**16**) the modification of the east-end of its side-chain was started (compounds **19a-d**). Together with the target sulfates **19a-d**, also their

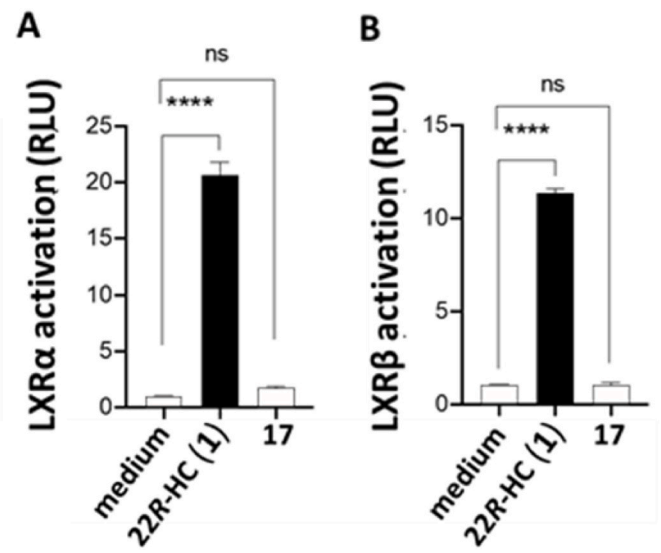

Fig. 6. Agonism profile of 22(*R*)-hydroxycholesterol-3-sulfate (**17**) towards LXRα and β. RLA, Relative Luciferase Activity. Compounds were dissolved in ethanol and tested at 10 μM. The results show mean ± SD of three biological samples. (n = 3/group). ****$p < 0.0001$; ns, not significant (ANOVA, Dunnett's multiple comparisons test).

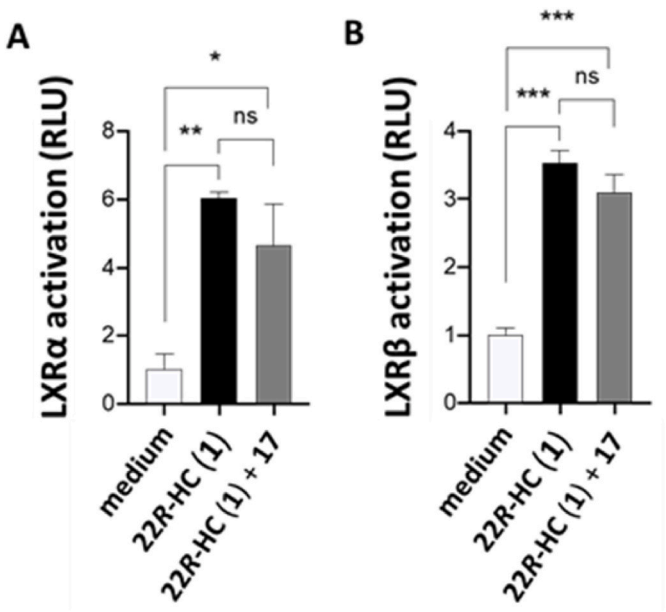

Fig. 7. Antagonism profile of 22(*R*)-hydroxycholesterol-3-sulfate (**17**) towards LXRα and β. RLA, Relative Luciferase Activity. Compound **17** was dissolved in ethanol and tested at 25 μM, 22*R*–HC (**1**) was instead tested at 10 μM. The results show mean ± SD of three biological samples. (n = 3/group). *$p < 0.05$, **$p < 0.01$, ***$p < 0.001$; ns, not significant (ANOVA, Tukey's multiple comparisons test).

corresponding parent non-sulfated derivatives, namely **18a-d**, were prepared and tested.

Any tested derivative was unable to activate LXRα (Fig. 8A) and β (Fig. 8B), thus confirming that the *S* stereochemistry at C-22 alone (compound **18a-d**) or along with the presence of the sulfate ester at C-3 (compounds **19a-d**) were structural features incompatible with an agonist profile regardless of the nature of the side-chain of the corresponding C-22-oxysterols. Then, we tested the potential antagonism exerted by **18a-d** and **19a-d** on the activation of LXRα (Fig. 9A) or β

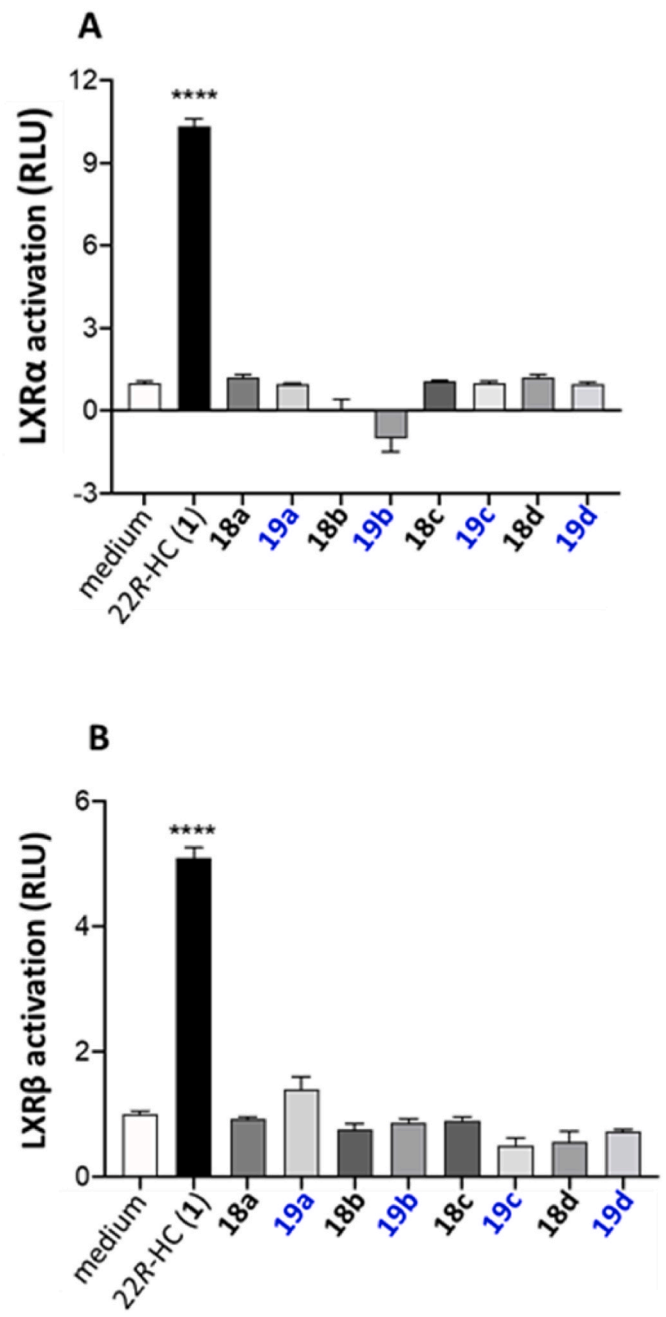

Fig. 8. Agonism profile of compounds **18a-d** and **19a-d** towards LXRα and β. RLA, Relative Luciferase Activity. Compounds were dissolved in ethanol and tested at 10 μM. The results show mean ± SD of three biological samples. (n = 3/group). ****$p < 0.0001$ (ANOVA, Dunnetts' multiple comparisons test).

induced (Fig. 9B) by 22*R*–HC (**1**).

All sulfated derivatives **19a-d** showed a very weak ability to inhibit the activation of LXRα; the corresponding non-sulfated parent derivatives **18a-d** gave similar poor results, apart from the benzyl derivative **18d**, in turn able to de-crease the activation evoked by 22*R*–HC (**1**) of more than 50 % (Fig. 9A). Regarding LXRβ (Fig. 9B) all sulfated derivatives **19a-d** were inactive; among the non-sulfated compounds, **18d** confirmed its antagonistic properties, shared by the ethyl derivative **18b**, too. Considering that the side-effects of LXR modulation have been generally lin-ked to the activation of α isoform, **18d** was considered a more interesting probe than **18b** due to its ability to inhibit LXRα to a greater extent than LXRβ. Dose-response curves gave very low micromolar IC_{50} values (2.04 μM for LXRα, and 1.58 μM for LXRβ) for **18d** (Fig. 10). Thus, the successful identification of 22(S)-23-phenyl-24-norchol-5-en-3β,22-diol (PFM046, **18d**) as a non-sulfated LXR antagonist, even more potent than PFM037 (**16**), allowed us to assume that the presence of the sulfate ester at C-3 was not an essential structural feature to ensure an antagonistic behavior to the corresponding 22(S)-hydroxy oxysterol. For antagonism, indeed, the presence of the C-3 sulfate moiety resulted only compatible with the iso-branched aliphatic side-chain typical of cholesterol, as in PFM037 (**16**). Albeit more potent than PFM037 (**16**), **18d** was endowed with a scarce isoform selectivity differently from PFM037 (**16**) virtually irrelevant as LXRβ antagonist (IC_{50} = 82.46 μM) [21].

The presence of an aromatic group at the level of **18d**'s side chain prompted us to continue the road of modifying the side-chain's east-end of 22(*S*)-oxysterols with a particular focus on the benzylic moiety of **18d**. The synthesis of a second series of derivatives was therefore designed with the aim to evaluate: a) the role played by the distance between C-22(*S*)-hydroxyl group and the aromatic ring in **18d** (**18e** and **18f**, respectively); b) the need to have an aromatic planar surface rather than a similarly sized alicyclic ring (**18g**); c) the influence of the introduction of a fluorine atom at the different position of the phenyl ring of **18d** (**18h-j**); d) the influence of the shift of the hydroxyl group of **18d** from C-22 to C-23 (**24** and **25**); e) the influence of the homologation of the side-chain of **18d** while maintaining the presence of the benzylic alcohol moiety (**22** and **23**). Moreover, the corresponding 22(*R*)-epimer and 22-keto analogue of **18d** were synthesized, **20** and **21**, respectively.

First, the ability of all the derivatives to act as LXRs agonists was assayed, obtaining comparable results on both isoforms (Fig. 11). As expected, all C-22-hydroxyl derivatives characterized by C-22(*S*)-configuration were inactive, as well as C-23-hydroxyl compounds, with the sole exception of **24**, which was able to weakly activate both LXRα and LXRβ. On the contrary the only C-22(*R*)-hydroxyl derivative present in this series, namely **20**, as well as its corresponding 22-keto derivative **21**, activated both LRXα and LXRβ to the same extent or better than 22*R*–HC (**1**), respectively. Once again, the *S* stereochemistry at C-22 showed to be incompatible with an agonist profile of the corresponding derivative regardless of the nature of the side-chain of the compound. Whereas the simple inversion of the stereochemistry at C-22 was enough to transform the potent LXR antagonist **18d** into the agonist **20**. A comparable effect was obtained by the oxidation of C-22-hydroxy group of **18d** leading to the agonist 22-keto derivative **21**.

Then, we moved to evaluate the antagonistic properties of the second series of derivatives hoping that some of the modifications performed on **18d** would have improved its profile as antagonist (Fig. 12). PFM037 (**16**) and **18d** were included as positive controls in the single-dose assays to facilitate the comparison of the new series of compounds respect to the antagonists in hands. As expected, the compounds **20**, **21**, and **24** already identified as agonists were unable to antagonize the activation promoted by 22*R*–HC (**1**), as well as **18e**. All the other derivatives showed antagonist properties on both isoforms. We decided to further evaluate the C-23(*S*)-hydroxy derivative **25** along with the three fluoro derivatives **18h-j**, because of their best performance in the single-dose assays, by measuring their IC_{50} values (Table 1).

The shift of the hydroxyl group from C-22 to C-23, while maintaining the side-chain length of **18d**, as in **25**, led to a weaker antagonist than **18d**. Comparable results were observed for the *ortho*-fluoro substituted analogue of **18d**, namely **18j**. The position of the introduction of the fluoro atom on the phenyl ring of **18d** had a great impact on the potency of the corresponding derivative; if, as seen, *ortho*-substitution was detrimental for potency, the contrary occurred in the case of the corresponding *meta*-fluoro derivative **18h**, more potent than **18d**, because endowed with IC_{50} values in the submicromolar range. The potency improvement of **18i**, respect to **18d**, was particularly evident on LXRβ. The *para*-substituted fluoro derivative **18i** was characterized by an intermediate potency, being weaker than **18h** and more potent than **18j**.

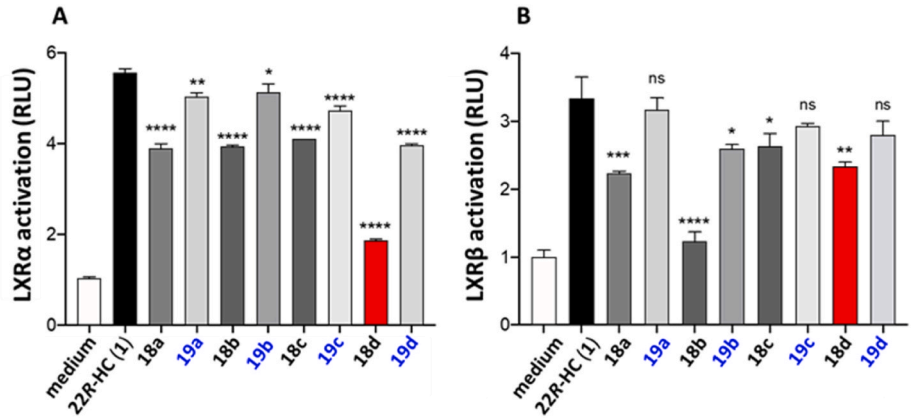

Fig. 9. Antagonist profile of compounds **18a-d** and **19a-d** towards LXRα and β. RLA, Relative Luciferase Activity. Compounds were dissolved in ethanol and used at 25 μM. LXRα and β activation was induced by 5 μM of 22*R*–HC (**1**). The results show mean ± SD of three biological samples. (n = 3/group). *$p < 0.05$, **$p < 0.01$, ***$p < 0.001$, ****$p < 0.0001$; ns, not significant (ANOVA, Dunnett's multiple comparisons test).

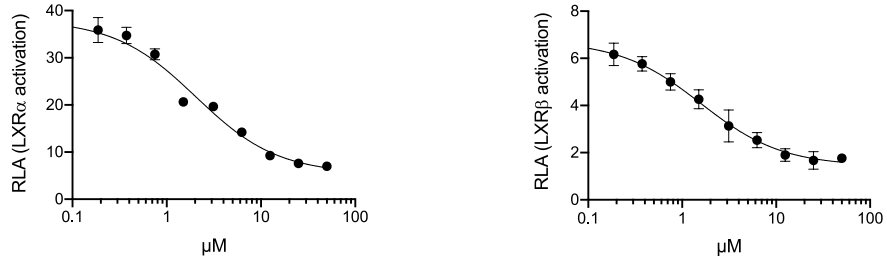

Fig. 10. Dose-response curves of the antagonist profile of compound PFM046 (**18d**) at LXRα (A) and β (B).

2.3. Gene expression profile of *18d*

On the basis of the results of the *in-vitro* luciferase-based reporter assays we deemed **18d** deserving of further characterization. Then, we tested by qPCR its ability to modulate common LXR target genes, such as ABCA1, SREBP1c, SCD1 and FASN in the U937 myeloid cells differentiated with PMA for 72 h and then treated with 22*R*–HC (**1**), the non-steroidal LXR agonist T0901317 or **18d**. As depicted in Fig. 13, **18d** did not induce SREBP-1c activation and inhibited the activation of SCD1 and FASN, recapitulating the behavior of our sulfated antagonist PFM037 (**16**), which we showed to inhibit SREBP-1c, SCD1 and FASN expression.[21] Unexpectedly, **18d** was able to significantly increase the expression of ABCA1 gene, differently from PFM037 (**16**), instead ineffective in the modulation of this LXR target gene.

2.4. In-vitro and in-vivo antitumor effects of PFM046 (*18d*)

According to our recent discovery about the remarkable antitumor responses observed *in-vivo* after PFM037 (**16**) administration,[21] we asked whether **18d** could be equally effective. Thus, murine B16F1 melanoma cells were treated for 72 h with **18d** (10 μM), observing a three-fold reduction of the cell number after 3 days (Fig. 14A). Analogous result was obtained on Lewis lung carcinoma (LLC) cells (Fig. 14B). Finally, we evaluated the *in-vivo* antitumor activity of **18d** in mice bearing the melanoma B16F1 or the lung cancer LLC. Our sulfated antagonist PFM037 (**16**) was included in the experiment to get reliable comparison data (Fig. 15). We were delighted to observe a significant reduction of the tumor volume in the mice treated with **18d** in both the tumor models. The new non-sulfated antagonist **18d** was as effective as the sulfated PFM037 (**16**), confirming that LXR antagonists are endowed with antitumor activity and are potentially exploitable for clinical

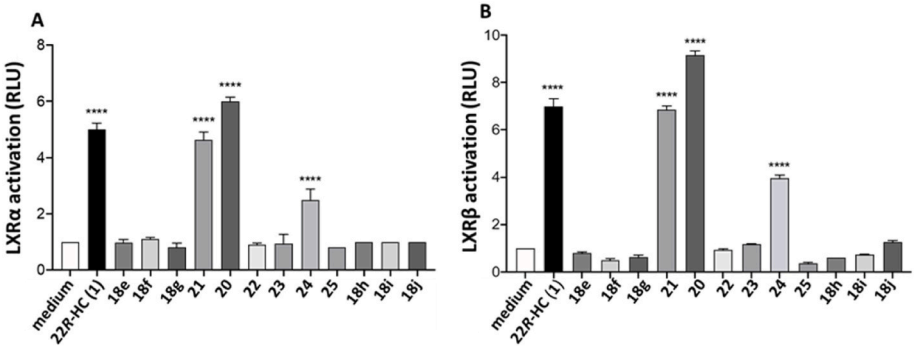

Fig. 11. Agonist profile of compounds **18e-j** and **20–25** towards LXRα and β. RLA, Relative Luciferase Activity. Compounds were dissolved in DMSO and tested at 10 μM. The results show mean ± SD of three biological samples. (n = 3/group). ****$p < 0.0001$ (ANOVA, Dunnett's multiple comparisons test).

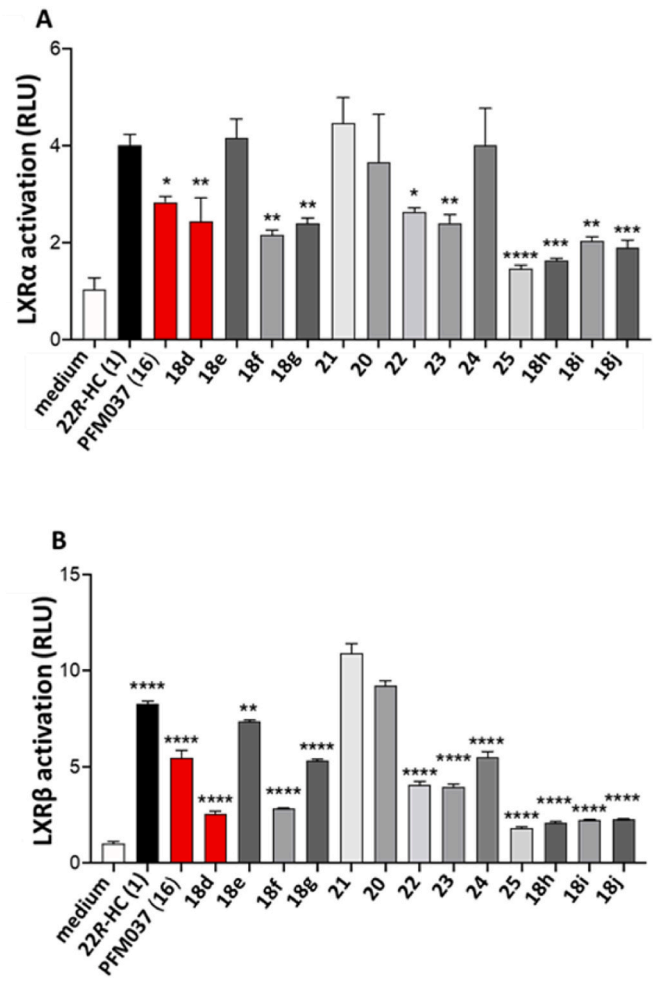

Fig. 12. Antagonist profile of compounds **18e-j** and **20**–**25** towards LXRα and β. RLA, Relative Luciferase Activity. Compounds were dissolved in DMSO and used at 25 μM. LXRα and β activation was induced by 5 μM of 22*R*–HC (**1**). The results show mean ± SD of three biological samples. (n = 3/group). $^{*}p < 0.05$, $^{**}p < 0.01$, $^{***}p < 0.001$, $^{****}p < 0.0001$ (ANOVA, Uncorrected Fisher's LSD test).

Table 1
IC_{50} values of the compounds **18d,h-j** and **25**.

Compound	LXRα IC_{50} (μM)	LXRβ IC_{50} (μM)
PFM037 (**16**)	5.18	82.46
PFM046 (**18d**)	2.04	1.58
25	8.63	12.59
18h	0.92	0.67
18i	4.64	3.97
18j	14.61	9.38

purposes.

2.5. *In-vitro and in-vivo antitumor pharmacokinetic (PK) studies of PFM046 (**18d**) and PFM037 (**16**)*

The most interesting compound of the series, namely PFM046 (**18d**), was characterized in *in-vitro* ADME assays, whose results are shown in Table 2. The same evaluation was also performed on PFM037 (**16**), not yet analysed under this aspect. PFM046 (**18d**) and PFM037 (**16**) showed a low solubility in PBS at pH 7.4, being characterized by calculated lipophilicity values of 5.76 and 6.49, respectively. By using chromatographic hydrophobicity index (CHI) method[26] logD could be not

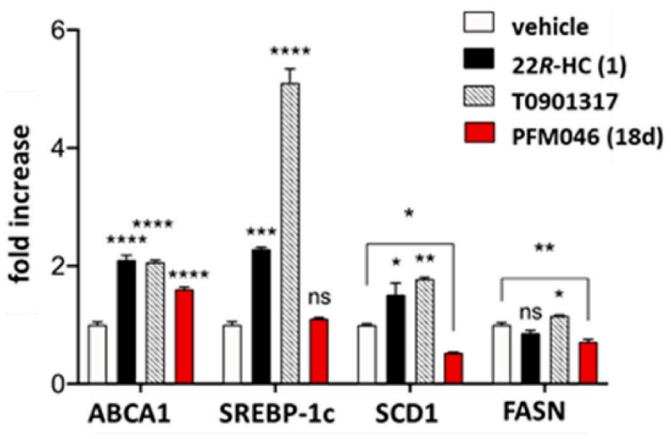

Fig. 13. Activation of LXR target genes by PFM046 (**18d**). U937 cells were treated with vehicle, 22*R*–HC (**1**) (5 μM), T0901317 (10 μM) or **18d** (10 μM). $^{****}p < 0.0001$, $^{***}p < 0.001$, $^{**}p < 0.01$, $^{*}p < 0.05$; ns, not significant (ANOVA, Sidak's multiple comparisons test).

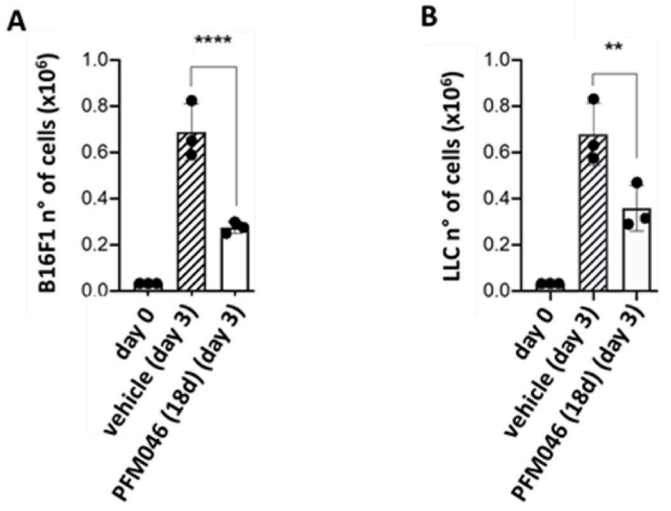

Fig. 14. Proliferation of B16F1 (A) and LLC (B) tumor cells in the presence of PFM046 (**18d**). **18d** (10 μM) was added to the cell cultures for 72 h. After that cells were collected and counted by trypan blue. The results show mean ± SD of three biological samples. (n = 3/group). $^{**}p < 0.01$, $^{****}p < 0.0001$ (ANOVA, Dunnett's multiple comparisons test).

determined. This was probably due to the combined effect of the low UV absorption and the high LogD values of the two compounds. In terms of plasma protein binding, both compounds proved to be able to interact to the protein with high affinity, thus leading to a contained unbound fraction that resulted not detectable after dialysis experiment. Hepatic intrinsic clearance (CLi) in liver microsomes highlighted a different behavior for the two compounds between the two species: PFM037 (**16**) showed a comparable moderate clearance in both human and mouse; on the contrary, PFM046 (**18d**) displayed a high clearance in mouse and low one in human On the basis of CLi results we assumed that the main isoform implicated in the metabolism of PFM037 (**16**) was CYP3A4, which is widely distributed in the two species, whereas a contribution from CYP2D6 cannot be ruled out in the case of PFM046 (**18d**). Indeed, CYP2D6 is more expressed in mouse than in human microsomes. The differences observed between the two derivatives are consistent with their corresponding side-chain structure as a matter of fact, the isopentyl side-chain of PFM037 (**16**) may represent a metabolic soft point for CYP3A4. On the other hand, the benzyl group present in PFM046 (**18d**) could protect the side-chain from the same metabolism.

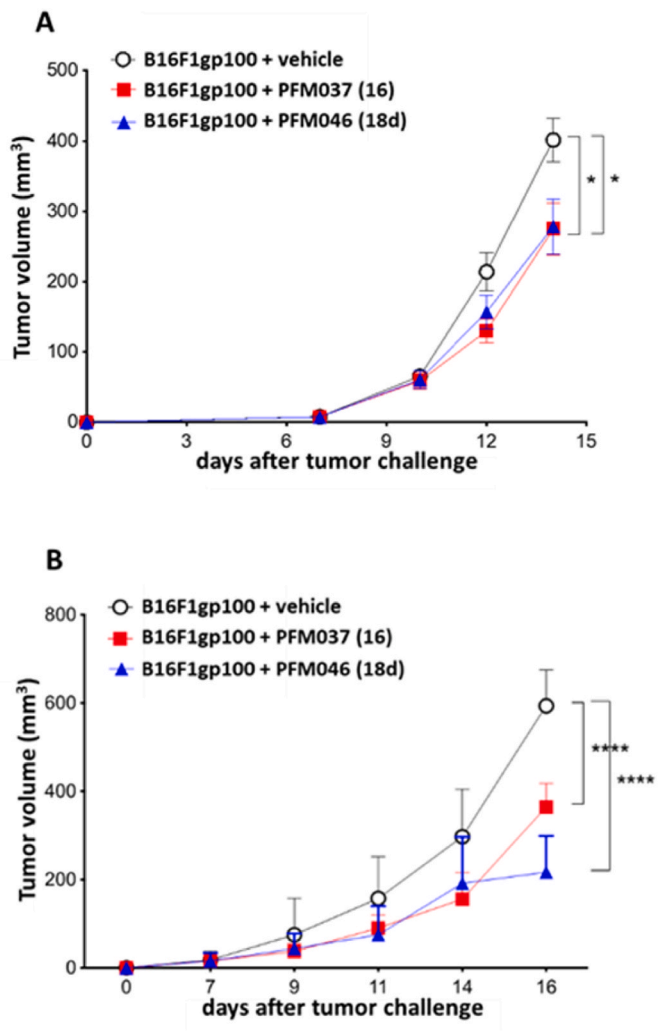

Fig. 15. *In-vivo* antitumor effects of PFM046 (**18d**) on B16F1 and LLC tumor models. Mice bearing established B16F1gp100 (**A**) or LLC (**B**) tumors were treated with **18d**, PFM037 (**16**) or vehicle and monitored for tumor growth. Mean ± SD of one experiment (n = 7/8 mice/group). *$p < 0.05$, ****$p < 0.0001$ (ANOVA, Dunnett's multiple comparisons test).

Table 2
In-vitro ADME assays for PFM037 (**16**) and PFM046 (**18d**).

	PFM037 (16)	PFM046 (18d)
kinetic solubility (pH 7.4), mg/mL	NO[a]	NO[a]
LogD (calculated)[b]	6.49	5.76
human plasma protein binding, (FU, %)	<1[c]	<1[c]
mouse plasma protein binding, (FU, %)	<1[c]	<1[c]
hepatic intrinsic clearance (CLi) in human liver microsomes(μL/min/mg protein)	26.4	<9.9
human WSM[d] *in-vivo* prediction	13.1	8.12
hepatic intrinsic clearance (CLi) in mouse liver microsomes (μL/min/mg protein)	17.2	45.8
mouse WSM[d] *in-vivo* prediction	41.4	70.1

[a] NQ: not quantifiable in PBS after 4 h of incubation.
[b] calculated using MarvinSketch Iodine.7, Version 21.15.7.
[c] value of receiver compart of dialysis was under the limit of quantitation, leading the information that compound is completely bind to the protein.
[d] WSM = well-stirred model.

For both compounds the calculated values of logD were found to be in agreement with the low solubility and very high protein binding observed, thus confirming the lipophilic nature of **18d** as discussed above, could be aided by the very high binding to the protein, in turn able to increase the concentration of the compound of interest after its *i.v.* administration. Furthermore, the high binding of the two compounds to the plasma proteins could increase their *in-vivo* half-life by increasing the exposure time, while protecting themselves from the liver metabolism. Accordingly, their preliminary ADME profile may suggest a hypothetical low dose associated to a high exposure/pharmacological effect.

To better understand the pharmacological effect of PFM037 (**16**) and PFM046 (**18d**) and to give support to the *in-vitro* ADME profiles, an *in-vivo* pharmacokinetic study was performed. Thus PFM037 (**16**) and PFM046 (**18d**) were administered in mouse C57BL/6 in the same conditions and dose used to test their antitumor effect. The data on the corresponding concentration at the different time points are reported in Table 3, and the corresponding PK parameters are reported in Table 4. PFM037 (**16**) showed a good profile, with a T_{max} observed at 1 h post-dosing and a C_{max} of 3170 ng/mL. Last time point detectable stood at 6 h. The total exposure was good with an average AUC_{last} of 4690 (h*ng/ml). A different profile was instead observed for PFM046 (**18d**): it reached a lower C_{max} in comparison to **16** up to 174 ng/mL and maintained a flat profile up to 24 h. Its AUC_{last} was though good and equal to 3070 (h*ng/ml).

Although PFM046 (**18d**) and PFM037 (**16**) showed different profiles, their exposures were in line with the biological effect highlighted by antitumor *in-vivo* experiments. The main difference between the two compounds was in terms of the time of effect (Fig. 16). Whereas PFM037 (**16**) showed a high peak of concentration followed by a rapid decrease, allowing to hypothesise a quick biological effect triggered by either high C_{max} or exposure, PFM046 (**18d**) showed a pretty flat profile, resulting into a biological effect more prolonged than PFM037 (**16**), but probably consequence of the high exposure. As supported from *in-vitro* data, the exposure confirmed a good distribution and, probably, a high distribution volume, which sustained the high level of concentration.

3. Conclusion

In summary, we carried out the first SAR study of sodium 22(*S*)-hydroxycholesterol-3-sulfate (PFM037, **16**), a steroidal LXR antagonist, which we have recently reported due its ability to improve anti-tumor immune response. The SAR study allowed us to establish that the presence of the hydroxyl group at C-22 endowed with *S* absolute configuration is the crucial factor for LXR antagonism of PFM037 (**16**) and in general for related oxysterols. Conversely, the presence of the sulfate moiety at C-3 is not an essential feature to ensure LXRs antagonism unless the compound is a cholestene derivative. Among 21 compounds prepared, we identified five non-sulfated LXRs antagonists with higher or comparable potency than PFM037 (**16**). Among them, 22(*S*)-23-phenyl-24-norchol-5-en-3β,22-diol (PFM046, **18d**) was selected for in-depth studies. In line with its antagonistic behavior, **18d** did not

Table 3
Average PK profile after i.p. administration of PFM037 (**16**) and PFM046 (**18d**) in mouse.

	PFM046 (18d)			PFM037 (16)		
Time	**Conc**	**SD**	**Conc**	**Conc**	**SD**	**Conc**
h	**ng/ml**	**ng/ml**	**nM**	**ng/ml**	**ng/ml**	**nM**
0	BQL	NC	NC	BQL	NC	NC
1	68.9	22.9	163	3170	1670	6290
3	109	99.8	259	363	241	720
6	110	18.7	262	65.2	41	129
24	167	70.3	396	BQL	NC	NC

The data are the mean of three animals; BQL: Below of quantitation limit; NC: not calculable.

Table 4
PK parameters after i.p. administration of PFM037 (**16**) and PFM046 (**18d**) in mouse.

	C_{max}	T_{max}	C_{last}	T_{last}	AUC_{last}	$AUC_{inf\ obs}$	$AUC\%_{extrap\ obs}$
	ng/ml	h	ng/ml	h	h[a]ng/ml	h[a]ng/ml	%
PFM037[a]	3170	1.0	65.2	6	4690	4800	2.5
SD[b]	1670	[1.0–1.0]	41	[6.0–6.0]	2600	2660	0.8
PFM046[a]	174	6.0	167	24	3070	NC	NC
SD[b]	67.7	[3.0–24]	70.3	[24–24]	909	NC	NC

The data are the mean of three animals.
[a] : for T_{max} and T_{last} median was used instead of mean.
[b] : for T_{max} and T_{last} range was used; AUC_{last}: area under the curve from the dosing to the last measurable time point; AUC_{inf}: area under the curve from the dosing extrapolated to infinity; AUC_%extrap_obs: percentage of AUC_{inf} due to extrapolation from T_{last} to infinity; NC: not calculable due to a flat profile.

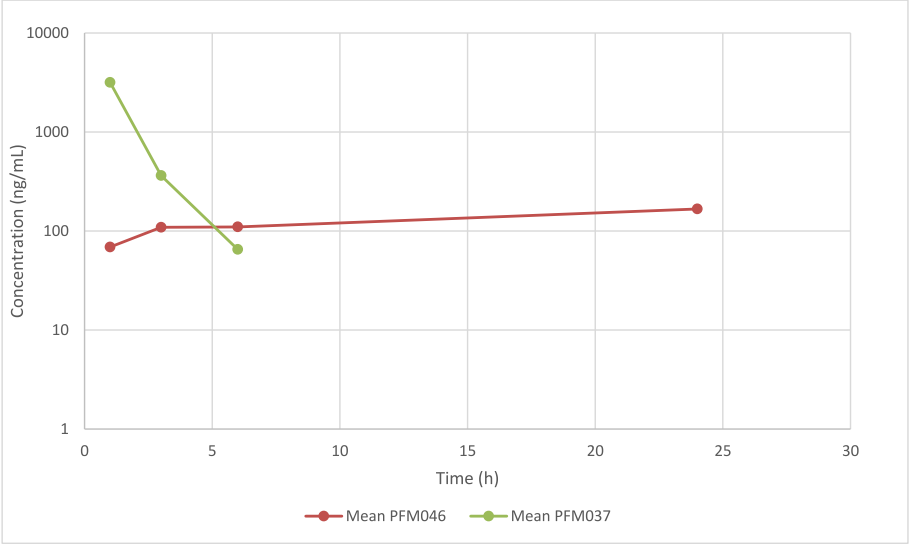

Fig. 16. Comparison of plasma profiles of PFM037 (**16**) and PFM046 (**18d**) after i.p. administration in mouse.

activate SREBP-1c and suppressed SCD1 and FASN expression. Unexpectedly **18d** significantly increased the expression of ABCA1 gene, differently from PFM037 (**16**), in turn ineffective in the modulation of this LXR target gene. Another difference between PFM046 (**18d)** and PFM037 (**16**) lies in their ability to delay proliferation of murine B16F1 melanoma cells as well as of LLC cells *in-vitro*: indeed, **18d** was effective in both the models, whereas PFM037 (**16**) did not show any direct effect on tumoral cell proliferation. Interestingly, PFM046 (**18d**) showed antitumor activity also *in-vivo* in comparable extend than PFM037 (**16**) in both cancer models. The preliminary ADME study fully supported the *in-vivo* antitumoral effect of **18d**, as well as PFM037 (**16**) confirming the well-established desirable physicochemical properties of the steroidal motif. The greater stability to human hepatic microsomes of PFM046 (**18d**) respect to PFM037 (**16**) constitutes another advantage to consider. We conclude that steroidal non-sulfated LXR antagonists, such as PFM046 (**18d**), are promising anticancer compounds that deserve further development and characterization.

4. Materials and methods

4.1. Chemistry

4.1.1. General methods

All reagents and solvents were reagent grade or were purified by standard methods before use. Anhydrous tetrahydrofuran (THF) was obtained by distillation from sodium-benzophenone ketyl; dichloromethane and diethyl ether from $LiAlH_4$; methanol from Mg turnings; toluene from sodium; acetonitrile from phosphorus(V) oxide; pyridine from CaH_2. Commercial solution of *n*-BuLi in hexanes was titrated with diphenylacetic acid before use.[27] All reactions requiring anhydrous conditions were performed under a positive argon atmosphere and all glassware was oven dried and/or flame dried.

Melting points (m.p.) were determined in open capillaries on a StuartTM SMP3 apparatus and are uncorrected.

^{1}H-, ^{13}C and ^{19}F NMR spectra were obtained on a Bruker AC 400 spectrometer as solutions in CDCl3 unless otherwise indicated. Chemical shifts were reported in parts per million (δ) and are referenced to residual protium in the deuterated solvent. The spin-spin coupling constants (*J*) were reported in Hertz (Hz) and refers to apparent multiplicities rather than true coupling constants. The spin multiplicities are indicated by the symbols s (singlet), d (doublet), t (triplet), q (quartet), m (multiplet), and bs (broad signal). Data are reported as: chemical shift, multiplicity, coupling constant, integration. Purification of the compounds were performed by flash column chromatography on silica gel 60 (230–400 mesh) or mpc on Merck LiChroprep Si 60 Lobar columns. Analytical thin-layer chromatography (TLC) was performed on TLC plates (silica gel 60 F254, aluminum foil). Compounds were detected under UV light or by 10 % phosphomolybdic acid in ethanol. Microanalyses were carried out on a Carlo Erba 1106 elemental analyzer, and the results were within ±0.4 % of the theoretical value. Purity was determined by microanalysis to be >95 % for all final compounds.

4.1.2. General procedure A – Grignard reaction with in situ generated organomagnesium reagents in THF

Few crystals of sublimated elemental iodine were added to a stirred suspension of grinded magnesium turnings (5.5 eq) in anhydrous THF (0.5 mL/mmol of Mg) kept under argon atmosphere at room

temperature. After 5 min a solution of the opportune alkyl bromide/chloride (5 eq) in anhydrous THF (0.5 mL/mmol of Mg) was added dropwise. After 1–3 h the resulting suspension was cooled to 0 °C and a solution of **26** or **27** (1 eq) in anhydrous THF (1.5 mL/mmol of Mg) was slowly added dropwise. As the addition was concluded, the system was allowed to warm to room temperature. After 15 h the reaction was quenched by the addition of an aqueous saturated solution of NH_4Cl and the resulting mixture was extracted with EtOAc. The combined organic layers were washed with brine and dried over anhydrous Na_2SO_4. After the removal of the volatiles at reduced pressure, the crude oily product was purified by flash chromatography (eluent: light petroleum/EtOAc, 9:1, v/v), unless otherwise indicated.

4.1.2.1. 22(S)-6β-methoxy-3α,5-cyclo-24-nor-5α-cholestan-22-ol (28c). Following general procedure A **28c** was obtained starting from **26** and 2-methyl-1-bromopropane in 51 % yield as an oil. ^{1}H NMR δ 0.32 (dd, J = 5.1 and 7.9 Hz, 1H), 0.54 (t, J = 4.6 Hz, 1H), 0.61 (s, 3H), 0.67–1.38 (m, 32H), 1.40–1.76 (m, 2H), 1.80–1.88 (m, 2H), 2.66 (s, 1H), 3.21 (s, 3H), 3.64–3.67 (m, 1H); ^{13}C NMR δ 11.48, 12.06, 12.97, 19.16, 21.30, 22.49, 22.67, 23.11, 24.01, 24.84 (2C), 27.71, 30.42, 33.21, 34.97, 35.05, 40.14, 40.42, 42.55, 43.22, 44.52, 47.84, 52.64, 56.26, 56.4, 71.18, 82.24.

4.1.2.2. 22(S)-6β-methoxy-24-phenyl-3α,5-cyclo-24-nor-5α-cholestan-22-ol (28d). Following general procedure A **28d** was obtained starting from **26** and benzyl bromide in 53 % yield as an oil. ^{1}H NMR δ 0.36 (dd, J = 5.1 and 7.8 Hz, 1H), 0.57 (t, J = 4.6 Hz, 1H), 0.63 (s, 3H), 0.71–1.96 (m, 29H), 2.55 (dd, J = 4.3 and 13.4 Hz, 1H), 2.69–2.76 (m, 2H), 3.25 (s, 3H), 3.82 (dd, J = 4.2 and 8.8 Hz, 1H), 7.12–7.16 (m, 3H), 7-21-7.25 (m, 2H); ^{13}C NMR δ 11.87, 12.07, 12.99, 19.20, 21.36, 22.71, 24.00, 24.86, 27.68, 30.44, 33.24, 34.95, 35.10, 40.15, 40.21, 41.99, 42.58, 43.26, 47.85, 52.64, 56.24, 56.47, 74.52, 82.27, 126.17, 128.42 (2C), 129.14 (2C), 139.44.

4.1.2.3. 22(S)-6β-methoxy-24-phenyl-3α,5-cyclo-5α-cholan-22-ol (28f). Following general procedure A **28f** was obtained starting from **26** and 1-bromo-2-phenylethane in 59 % yield as an oil. ^{1}H NMR δ 0.46 (m, 1H), 0.67 (m, 1H), 0.74 (s, 3H), 0.87–2.05 (m, 29H), 2.60–2.79 (m, 3H), 3.35 (s, 3H), 3.73 (m, 1H), 7.18–7.34 (m, 5H). ^{13}C NMR δ 11.57, 12.12, 13.00, 19.20, 21.36, 22.70, 24.03, 24.86, 27.63, 30.44, 32.88, 33.24, 34.96, 35.10, 37.21, 40.17, 40.40, 42.59, 43.26, 47.85, 52.60, 56.27, 56.47, 73.09, 82.27, 125.68, 127,39, 128.28 (2C), 142.14.

4.1.2.4. 22(S)-6β-methoxy-23-cyclohexyl-3α,5-cyclo-24-nor-5α-cholan-22-ol (28g). Following general procedure A **28g** was obtained starting from **26** and (bromomethyl)cyclohexane in 69 % yield as an oil (eluent light petroleum/EtOAc, 93:7, v/v). ^{1}H NMR δ 0.38 (dd, J = 5.13 and 7.92 Hz, 1H), 0.60 (t, J = 4. 61 Hz, 1H), 0.67 (s, 3H), 0.73–1.93 (m, 40H), 2.73 (m, 1H), 3.28 (s, 3H), 3.75 (m, 1H). ^{13}C NMR δ 11.42, 11.97, 12.89, 19.06, 20.80, 22.59, 23.92, 24.73, 25.39, 26.05, 26.17, 26.43, 27.62, 30.32, 33.12, 33.87, 34.27, 34.87, 34.95, 40.05, 40.81, 42.43, 43.12, 43.17, 47.76, 52.56, 56.16, 56.32, 70.35, 82.15.

4.1.2.5. 22(S)-6β-methoxy-23-(3′-fluorophenyl)-3α,5-cyclo-24-nor-5α-cholan-22-ol (28h). Following general procedure A, **28h** was obtained starting from **26** and 2-fluorobenzyl bromide as an oil. The product resulted contaminated by co-eluting impurities.

4.1.2.6. 22(S)-6β-methoxy-23-(4′-fluorophenyl)-3α,5-cyclo-24-nor-5α-cholan-22-ol (28i). Following general procedure A, **28i** was obtained starting from **26** and 3-fluorobenzyl bromide as an oil. The product resulted contaminated by co-eluting impurities.

4.1.2.7. 22(S)-6β-methoxy-23-(2′-fluorophenyl)-3α,5-cyclo-24-nor-5α-cholan-22-ol (28j). Following general procedure A, **28j** was obtained starting from **26** and 4-fluorobenzyl bromide in 76 % yield as an oil. ^{1}H NMR δ 0.37 (m, 1H), 0.59 (m, 1H), 0.63 (s, 3H), 0.66–1.98 (m, 27H), 2.53 (dd, J = 3.82 and 11.80 Hz, 1H), 2.68–2.74 (m, 2H), 3.26 (s, 3H), 3.80, (m, 1H), 6.89–6.94 (m, 2H), 7.08–7.11 (m, 2H). ^{13}C NMR δ 11.41, 11.83, 13.06, 19.24, 21.00, 22.75, 23.84, 24.03, 24.90, 27.74, 33.30, 35.01, 35.13, 40.16, 41.10, 42.65, 43.31, 47.91, 52.66, 56.30, 56.51, 74.68, 82.35, 115.21 (2C, d, J = 20.90 Hz), 126.28, 126.40, 130.52 (d, J = 7.60 Hz), 135.14, 161.48 (d, J = 242.4 Hz). ^{19}F NMR (376 MHz, CDCl3):

δ −117.44.

4.1.2.8. 22(S)-6β-methoxy-3α,5-cyclo-5α-cholestan-22-ol (28k). Following general procedure A, **28k** was obtained starting from **26** in 66 % yield as an oil. ^{1}H NMR δ 0.43 (s, 1H), 0.65 (s, 1H), 0.73 (s, 3H), 0.74–1.99 (m, 38H), 2.77 (s, 1H), 3.32 (s, 3H), 3.63 (s, 1H). ^{13}C NMR δ 11.43, 12.17, 13.04, 19.26, 21.43, 22.54, 22.69, 22.76, 24.09, 24.92, 27.79, 28.17, 30.52, 33.19, 33.30, 35.03, 35.18, 35.63, 40.12, 40.24, 42.66, 43.33, 47.93, 52.67, 56.36, 56.54, 73.88, 82.35.

4.1.2.9. 23(S)- and 23(R)-6β-methoxy-24-phenyl-3α,5-cyclo-5α-cholan-23-ol (34) and (35). Following general procedure A, **34** and **35** were obtained starting from **27** and benzyl bromide in 51 % overall yield (eluent light petroleum/EtOAc, 85:15, v/v). **34**: (wax) ^{1}H NMR δ 0.38 (dd, J = 5.18 and 7.76 Hz, 1H), 0.60 (m, 1H), 0.69 (s, 3H), 0.70–1.98 (m, 29H), 2.44 (dd, J = 9.07 and 13.55 Hz, 1H), 2.72 (m, 1H), 2.87 (dd, J = 2.90 and 13.66 Hz, 1H), 3.28 (s, 3H), 3.86 (m, 1H), 7.13–7.30 (m, 5H). ^{13}C NMR δ 12.23, 13.04, 19.25, 19.36, 21.42, 22.73, 24.12, 24.92, 25.56, 28.48, 30.43, 33.30, 33.90, 35.00, 35.19, 40.25, 42.83, 43.32, 43.58, 47.92, 56.42, 56.53, 57.00, 71.41, 82.35, 126.42, 128.53 (2C), 129.41 (2C), 138.62. **35**: (oil) ^{1}H NMR δ 0.38 (dd, J = 5.21 and 7.92 Hz, 1H), 0.59 (m, 1H), 0.69 (s, 3H), 0.70–1.98 (m, 29H), 2.63 (m, 2H), 2.72 (m, 1H), 3.27 (s, 3H), 3.86 (m, 1H), 7.14–7.31 (m, 5H). ^{13}C NMR δ 12.25, 12.98, 18.44, 19.23, 21.43, 22.68, 24.08, 24.89, 28.40, 30.36, 32.44, 33.26, 34.91, 35.22, 40.25, 42.84, 43.29 (2C), 45.20, 47.90, 56.46 (2C), 56.80, 69.67, 126.30, 128.43 (2C), 129.32 (2C), 138.68.

4.1.3. General procedure B – Grignard reaction with a commercial solution of organomagnesium reagents in THF

A solution of **26** or **27** (1 eq) in THF (10 mL/mmol) was added dropwise to a stirred solution of 3 M alkyl magnesium bromide in THF (5 eq) kept under argon atmosphere at 0 °C. As the addition was concluded, the system was allowed to warm to room temperature. After 15 h the reaction was quenched by the addition of an aqueous saturated solution of NH_4Cl and the resulting mixture was extracted with EtOAc. The combined organic layers were washed with brine and dried over anhydrous Na_2SO_4. After the removal of the volatiles at reduced pressure, the crude oily product was purified by flash chromatography (eluent: light petroleum/EtOAc, 90:10, v/v), unless otherwise indicated.

4.1.3.1. 22(S)-6β-methoxy-3α,5-cyclo-24-nor-5α-cholan-22-ol (28a). Following general procedure B **28a** was obtained starting from **26** and methylmagnesium chloride in 50 % yield as an oil. ^{1}H NMR δ 0.34 (s, 1H), 0.55 (s, 1H), 0.63 (s, 3H), 0.65–2.00 (m, 30H), 2.68 (s, 1H), 3.23 (s, 3H), 3.84 (m, 1H); ^{13}C NMR δ 11.21, 12.12, 13.01, 19.22, 21.39, 22.72, 24.09, 24.88, 27.70, 30.47, 33.27, 34.98, 35.15, 40.19, 41.71, 42.62 (2C), 43.29, 47.89, 52.83, 56.28, 56.49, 69.13, 82.31.

4.1.3.2. 22(S)-6β-methoxy-3α,5-cyclo-5α-cholan-22-ol (28b). Following general procedure B **28b** was obtained starting from **26** and ethylmagnesium chloride in 70 % yield as an oil. ^{1}H NMR δ 0.34 (dd, J = 5.1 and 7.9 Hz, 1H), 0.56 (t, J = 4.2 Hz, 1H), 0.64 (s, 3H), 0.71–0.83 (m, 18H), 0.85–1.90 (m, 14H), 2.68 (s, 1H), 3.23 (s, 3H), 3.46–3.49 (m, 1H); ^{13}C NMR δ 10.84, 11.35, 12.11, 13.00, 19.22, 21.38, 22.72, 24.05, 24.88, 27.75, 28.05, 30.47, 33.26, 34.98, 35.13, 39.69, 40.19, 42.61, 43.28, 47.88, 52.59, 56.32, 56.49, 75.09, 82.31.

4.1.3.3. 22(S)-6β-methoxy-3α,5-cyclo-5α-cholan-22-ol (28e). Following general procedure B **28e** was obtained starting from **26** and phenylmagnesium chloride. The compound **28e** obtained after flash chromatography was in large extent contaminated. The large amounts of impurities hampered the reading of the NMR spectra thus avoiding the identification of the peaks of the desired product.

4.1.3.4. (23R)- + (23S)-6β-methoxy-23-phenyl-3α,5-cyclo-24-nor-5α-cholan-23-ols (36 + 37). Following general procedure B **36** + **37** were obtained starting from **27** and phenylmagnesium bromide in 72 % yield (eluent light petroleum/EtOAc, 85:15, v/v). ^{1}H NMR δ 0.34 (m, 1H), 0.56 (s, 1.5H, CH_3 of isomer A), 0.56 (m, 1H), 0.60–2.00 (m, 30.5H), 2.67 (m, 1H), 3.22 (s, 1.5H, CH_3 of isomer A), 3.23 (s, 1.5H, CH_3 of isomer B), 4.66 (dd, J = 5.61 and 8.89 Hz, 0.5H, CH of isomer A), 4.71 (dd, J = 2.28 and 10.44 Hz, 0.5H, CH of isomer B), 7.18–7.29 (m, 5H). ^{13}C NMR δ 12.06, 12.33, 13.03, 18.49, 19.24, 19.37, 21.42, 22.69, 24.05, 24.92, 28.29, 28.45, 30.37, 32.94, 33.30, 33.44, 34.96, 35.17, 35.25, 40.20, 40.30, 42.74, 42.93, 43.30, 45.04, 46.33, 47.93, 56.42, 56.51, 56.79, 71.50, 73.64, 82.34, 125.50, 126.33, 127.22, 127.69, 128.38, 128.49, 144.51, 145.98.

4.1.4. General procedure C – Acetylation of C-22-hydroxy group

Acetic anhydride (2 eq) and 4-DMAP (0.25 eq) were added to a stirred solution of the alcohol (1 eq) in CH_2Cl_2 (12 mL/mmol) and pyridine (0.15 mL/mmol) kept at room temperature. After 24 h, a solution of 3 M HCl was added, the organic layer was separated and washed with H_2O, brine and then dried over anhydrous Na_2SO_4. After the removal of the volatiles at reduced pressure, the crude product was used as such for the next step (see general procedure D), unless otherwise indicated.

4.1.4.1. 22(S)-6β-methoxy-3α,5-cyclo-24-nor-5α-cholan-22-yl acetate (41a). Following general procedure C, **41a** was obtained starting from **28a** in 70 % yield as an oil; ^{1}H NMR δ 0.29 (m, 1H), 0.51 (m, 1H), 0.58 (s, 3H), 0.59–1.90 (m, 32H), 2.63, (s, 1H), 3.19 (s, 3H), 4.90 (m, 1H); ^{13}C NMR δ 11.95, 12.57, 12.91, 17.72, 19.14, 21.15, 21.32, 22.65, 23.96, 24.81, 27.76, 30.36, 33.20, 34.77, 35.10, 40.06, 40.56, 42.46, 43.18, 47.82, 52.61, 56.18, 56.39, 72.43, 82.18, 170.63.

4.1.4.2. 22(S)-6β-methoxy-3α,5-cyclo-5α-cholan-22-yl acetate (41b). Following general procedure C, **41b** was obtained starting from **28b** in 85 % yield as an oil. ^{1}H NMR δ 0.25 (dd, J = 5.1 and 7.8 Hz, 1H), 0.45 (t, J = 4.5 Hz, 1H), 0.53 (s, 3H), 0.54–1.70 (m, 31H), 1.95 (s, 3H), 2.58 (brs, 1H), 3.12 (s, 3H), 4.70 (t, J = 6.7 Hz, 1H); ^{13}C NMR δ 10.06, 11.66, 12.31, 12.75, 18.94, 20.78, 21.12, 22.46, 23.78, 24.61, 24.73, 27.84, 30.16, 33.01, 34.59, 34.87, 38.26, 39.89, 42.30, 42.98, 47.61, 52.31, 56.05, 56.13, 77.25, 82.01, 170.55.

4.1.4.3. 22(S)-6β-methoxy-3α,5-cyclo-24-nor-5α-cholestan-22-yl acetate (41c). Following general procedure C, **41c** was obtained starting from **28c** in 91 % yield as an oil. ^{1}H NMR δ 0.25 (dd, J = 5.2 and 7.8 Hz, 1H), 0.45 (t, J = 4.5 Hz, 1H), 0.56 (s, 3H), 0.57–1.92 (m, 38H), 2.58 (s, 1H), 3.12 (s, 3H), 4.70 (t, J = 6.7 Hz, 1H); ^{13}C NMR δ 11.86, 12.77, 12.92, 19.14, 21.08, 21.32, 22.52, 22.67 (2C), 24.00, 24.64, 24.81, 28.08, 30.35, 33.21, 34.78, 35.08, 39.40, 40.07, 41.22, 42.52, 43.18, 47.82, 52.60, 56.22, 56.38, 74.42, 82.23, 170.67.

4.1.4.4. 22(S)-23-phenyl-6β-methoxy-3α,5-cyclo-24-nor-5α-cholan-22-yl acetate (41d). Following general procedure C **41d** was obtained starting from **28d** in 65 % yield as an oil. ^{1}H NMR δ 0.34 (m, 1H), 0.55 (m, 4H), 0.70–1.90 (m, 29H), 2.66 (m, 2H), 2.83 (m, 1H), 3.22 (s, 3H), 5.13 (m, 1H), 7.11–7.18 (m, 5H); ^{13}C NMR δ 11.85, 12.80, 12.97, 19.20, 21.01, 21.43, 22.70, 23.99, 24.89, 28.05, 30.41, 33.29, 34.83, 35.22, 38.05, 38.30, 40.16, 42.59, 43.26, 47.92, 52.62, 56.34, 56.46, 76.83, 82.28, 126.21, 128.29 (2C), 129.15 (2C), 137.90, 170.43.

4.1.5. General procedure D – removal of the 6β-methoxy-3α,5-cycloprotection by acidic hydrolysis

p-Toluenesulfonic acid monohydrate (0.3 eq) was added to a stirred solution of the cyclosterol (1 eq) in 1,4-dioxane (28 mL/mmol) and water (9 mL/mmol) kept at room temperature. The resulting mixture was warmed to 75 °C (external temperature) and stirred for 1.5–2.5 h. The reaction was quenched by diluting with water and extracting with EtOAc. The combined organic layers were washed with brine and dried over anhydrous Na_2SO_4. After the removal of the volatiles at reduced pressure, the crude oily product was purified by flash chromatography (eluent: light petroluem/EtOAc, 70:30, v/v), unless otherwise indicated.

4.1.5.1. 22(S)-24-norchol-5-en-3β,22-diol (18a). Following general procedure D **18a** was obtained starting from **28a** in 51 % yield as a white solid. M.p. 204–206 °C; ^{1}H NMR (DMSO-d_6) δ 0.63 (m, 3H), 0.80–2.10 (m, 31H), 3.70 (s, 1H), 4.00 (s, 1H), 4.55 (s, 1H), 5.25 (s, 1H). ^{13}C NMR (DMSO-d_6) δ 12.19, 19.69, 21.21, 22.14, 24.46, 27.75, 31.94, 32.06, 36.60, 37.45, 42.16, 42.33, 42.75, 50.17, 52.70, 56.81, 67.24, 70.5, 120.99, 141.78. Anal. calcd for ($C_{23}H_{38}O_2$): C, 79.71 %; H, 11.05 %. Found: C, 80,00 %; H, 11.10 %.

4.1.5.2. 22(S)-Chol-5-en-3β,22-diol (18b). Following general procedure D **18b** was obtained starting from **28b** in 52 % yield as a white solid. M.p. 211–213 °C; ^{1}H NMR (DMSO-d_6) δ 0.54 (m, 3H), 0.60–2.10 (m, 32H), 3.16 (m, 1H), 3.23 (m, 1H), 3.96 (s, 1H), 4.56 (s, 1H), 5.16 (s, 1H). ^{13}C NMR (DMSO-d_6) δ 11.67, 12.21, 12.31, 19.71, 21.24, 24.45, 27.85, 28.32, 31.96, 32.08, 36.62, 37.49, 42.18, 42.77, 50.21, 52.50, 56.90, 70.58, 73.39, 121.01, 141.79. Anal. calcd for ($C_{24}H_{40}O_2$): C, 79.94 %; H, 11.18 %. Found: C, 80.42 %; H, 11.25 %.

4.1.5.3. 22(S)-24-Norcholest-5-en-3β,22-diol (18c). Following general procedure D **18c** was obtained starting from **28c** in 50 % yield as a white solid. M.p. 200–202 °C; ^{1}H NMR (DMSO-d_6) δ 0.51 (s, 3H), 0.66–2.00 (s, 37H), 3.13 (m, 1H), 3.90 (m, 1H), 4.58 (m, 1H), 5.14 (s, 1H). ^{13}C NMR (DMSO-d_6) δ 12.36, 12.61, 19.88, 21.38, 23.25, 23.89, 24.60, 25.14, 28.04, 32.03, 32.13, 32.27, 36.79, 37.63, 41.22. 42.37, 42.81, 45.04, 50.40, 52.80, 57.04, 69.69, 70.80, 121.25, 141.95. Anal. calcd for ($C_{26}H_{44}O_2$): C, 80.35 %; H, 11.41 %. Found: C, 80.63 %; H, 11.51 %.

4.1.5.4. 22(S)-23-phenyl-24-norchol-5-en-3β,22-diol (18d). Following general procedure D **18d** was obtained starting from **28d** in 59 % yield as a white solid. M.p. 181–183 °C; ^{1}H NMR (DMSO-d_6) δ 0.46 (m, 3H), 0.80–1.98 (m, 26H), 1.99–2.03 (m, 2H), 2.56–2.58 (m, 1H), 3.15 (brs, 1H), 3.60 (m, 1H), 4.18 (m, 1H), 4.55 (m, 1H), 5.15 (brs, 1H), 7.0-7-16 (m, 5H); ^{13}C NMR δ 11.70, 11.91, 19.35, 21.06, 24.13, 27.65, 31.5, 31.78, 31.88, 36.42, 37.21, 39.73, 40.21, 42.03, 42.20 (2C), 50.04, 52.56, 56.58, 71.66, 74.60, 121.54, 126.23, 128.48 (2C), 129.17 (2C), 139.43, 140.75. Anal. calcd for ($C_{29}H_{42}O_2$): C, 82.41 %; H, 10.02 %. Found: C, 82.64 %; H, 10.41 %.

4.1.5.5. 22(S)-22-phenyl-23,24-dinorchol-5-en-3β,22-diol (18e). Following general procedure D **18e** was obtained starting from the impure **28e** in 34 % yield (overall yield from **26**) as a white solid. M.p. = 233–236 °C (with decomposition). ^{1}H NMR δ 0.72 (s, 3H), 0.77 (d, J = 6.52 Hz, 3H), 0.98–2.30 (m, 26H), 3.53 (m, 1H), 4.95 (s, 1H), 5.38 (s, 1H), 7.24–7.37 (m, 5H). ^{13}C NMR δ 11.08, 11.76, 19.39, 21.06, 24.30, 28.28, 31.64, 31.85, 31.97, 36.48, 37.21, 39.64, 42.32, 43.38, 50.04, 52.68, 56.79, 71.78, 75.11, 121.62, 125.50 (2C), 126.54, 127.98 (2C), 140.78, 144.45. Anal. calcd for ($C_{28}H_{40}O_2$): C, 82.30 %; H, 9.87 %. Found: C, 82.60 %; H, 10.01 %.

4.1.5.6. 22(S)-24-phenylchol-5-en-3β,22-diol (18f). Following general procedure D **18f** was obtained starting from **28f** in 82 % yield as a white solid. M.p. = 186–187 °C. ^{1}H NMR δ 0.70 (s, 3H), 0.93 (d, J = 5.94 Hz, 3H), 1.00–2.00 (m, 26H), 2.21–2.33 (m, 2H), 2.64 (ddd, J = 6.07, 10.00

and 13.84 Hz, 1H), 2.78 (ddd, J = 5.87, 10.50 and 13.81 Hz, 1H), 3.50–3.57 (m, 1H), 3.73 (m, 1H), 5.36 (m, 1H), 7.20–7.32 (m, 5H). ^{13}C NMR δ 11.65, 11.78, 19.38, 21.06, 24.19, 27.63, 31.60, 31.81, 31.90, 32.95, 36.44, 37.19, 37.28, 39.74, 40.48, 42.23 (2C), 50.00, 52.53, 56.60, 71.75, 73.23, 121.62, 125.78, 128.36 (2C), 140.73, 142.19. Anal. calcd for ($C_{30}H_{44}O_2$): C, 82.52 %; H, 10.16 %. Found: C, 82.70 %; H, 10.22 %.

4.1.5.7. 22(S)-23-Cyclohexyl-24-norchol-5-en-3β,22-diol (18g). Following general procedure D **18g** was obtained starting from **28g** in 66 % yield as a white solid. M.p. = 180–182 °C. ^{1}H NMR δ 0.70 (s, 3H), 0.90–2.05 (m, 40H), 2.21–2.31 (m, 2H), 3.52 (m, 1H), 3.81 (m, 1H), 5.36 (s, 1H). ^{13}C NMR δ 11.63, 11.78, 19.39, 21.09, 24.21, 26.24, 26.36, 26.61, 27.74, 31.62, 31.84, 31.93, 33.32, 34.06, 34.53, 36.46, 37.22, 39.76, 40.70, 42.23 (2C), 43.38, 50.06, 52.68, 56.61, 70.76, 71.77, 121.64, 140.75. Anal. calcd for ($C_{29}H_{48}O_2$): C, 81.25 %; H, 11.29 %. Found: C, 81.60 %; H, 11.35 %.

4.1.5.8. (22S)-23-(3′-Fluorophenyl)-24-norchol-5-en-3β,22-diol (18h). Following general procedure D **18h** was obtained starting from **28h** in 50 % yield as a white solid (eluent: light petroleum/EtOAc, 65:35, v/v). M.p. = 177–178 °C. ^{1}H NMR ($CDCl_3$+CD_3OD) δ 0.65 (s, 3H), 0.80–2.30 (m, 29H), 2.74–2.79 (m, 2H), 3.49 (m, 1H), 3.93 (m, 1H), 5.33 (m, 1H), 7.01–7.08 (m, 2H), 7.20–7.22 (m, 2H). ^{13}C NMR ($CDCl_3$+CD_3OD) δ 11.73, 11.84, 19.36, 21.08, 24.16, 27.69, 31.42, 31.81, 31.91, 36.46, 37.23, 39.76, 40.27, 41.71, 42.08, 42.24, 50.06, 52.52, 56.63, 71.56, 74.38, 113. 10 (d, J = 21 Hz), 115.98 (d, J = 21 Hz), 121.56, 124.85, 129.84 (d, J = 8 Hz), 140.79, 142.19 (d, J = 8 Hz). ^{19}F NMR ($CDCl_3$+CD_3OD) δ −120.65. Anal. calcd for ($C_{29}H_{41}FO_2$): C, 79.05 %; H, 9.38 %. Found: C, 80.00 %; H, 9.50 %.

4.1.5.9. (22S)-23-(4′-Fluorophenyl)-24-norchol-5-en-3β,22-diol (18i). Following general procedure D **18**i was obtained starting from **28i** in 85 % yield as a white solid. M.p. = 176–179 °C. ^{1}H NMR ($CDCl_3$+CD_3OD) δ 0.61 (s, 3H), 0.85–2.00 (m, 27H), 2.15–2.25 (m, 2H), 2.57 (dd, J = 3.82 and 13.44 Hz, 1H), 2.76 (dd, J = 9.20 and 13.64 Hz, 1H), 3.47 (m, 1H), 3.84 (m, 1H), 5.29 (m, 1H), 6.90 (m, 3H), 7.20 (m, 1H). ^{13}C NMR ($CDCl_3$+CD_3OD) δ 11.71, 11.86, 19.35, 21.02, 24.12, 27.65, 31.55, 31.77, 31.87, 36.41, 37.16, 39.69, 40.30, 41.73, 42.20 (2C), 49.98, 52.50, 56.54, 71.71, 74.45, 113.14 (d, J = 20.90 Hz), 115.96 (d, J = 20.70 Hz), 121.57, 124.80, 129.85 (d, J = 8.30 Hz), 140.70, 142.04, 162.86 (d, J = 244.00 Hz). ^{19}F NMR δ −113.90. Anal. calcd for ($C_{29}H_{41}FO_2$): C, 79.05 %; H, 9.38 %. Found: C, 80.03 %; H, 9.52 %.

4.1.5.10. (22S)-23-(2′-Fluorophenyl)-24-norchol-5-en-3β,22-diol (18j). Following general procedure D **18j** was obtained starting from **28j** in 50 % yield as a white solid (eluent: light petroleum/EtOAc, 55:45, v/v). M. p. = 172–174 °C. ^{1}H NMR ($CDCl_3$+CD_3OD) δ 0.65 (s, 3H), 0.75–2.20 (m, 29H), 2.45–2.60 (m, 1H), 2.75–2.85 (m, 2H), 3.90 (m, 1H), 5.29 (m, 1H), 7.00–7.15 (m, 2H), 7.16–7.20 (m, 2H). ^{13}C NMR ($CDCl_3$+CD_3OD) δ 11.71, 11.86, 14.16, 19.36, 21.04, 24.13, 27.67, 31.57, 31.78, 31.87, 36.42, 37.18, 39.71, 40.12, 41.10, 42.21 49.99, 52.52, 56.56, 71.72, 74.68, 115.25 (d, J = 20.90 Hz), 121.58, 130.52 (d, J = 7.50 Hz), 135.06, 140.72, 161.50 (d, J = 242.60 Hz). ^{19}F NMR δ −117.48. Anal. calcd for ($C_{29}H_{41}FO_2$): C, 79.05 %; H, 9.38 %. Found: C, 80.04 %; H, 9.52 %.

4.1.5.11. 3β-hydroxy-23-phenyl-24-norchol-5-en-22-one (21). Following general procedure D **21** was obtained starting from **31** in 88 % yield as a white solid. M.p. = 167–168 °C. ^{1}H NMR δ 0.68 (s, 3H), 1.08–2.00 (m, 27H), 2.59–2.70 (m, 1H), 3.49–3.56 (m, 1H), 3.72 (s, 2H), 5.45 (m, 1H), 7.19–7.35 (m, 5H). ^{13}C NMR δ 12.04, 16.65, 19.38, 21.00, 24.47, 27.49, 31.60, 31.84, 36.46, 37.21, 39.59, 42.24, 42.52, 48.68, 48.82, 50.02, 51.95, 56.03, 71.72, 121.55, 126.86, 128.52 (2C), 129.63 (2C), 134.08, 140.70, 211.52. Anal. calcd for ($C_{29}H_{40}O_2$): C, 82.81 %; H, 9.59 %. Found: C, 82.98 %; H, 10.05 %.

4.1.5.12. 23(S)-24-phenylchol-5-en-3β,23-diol (22). Following general procedure D **22** was obtained starting from **34** in 73 % yield as a white solid (eluent: light petroleum/EtOAc, 75:25, v/v). M.p. = 182–183 °C. ^{1}H NMR δ 0.66 (s, 3H), 0.96–2.00 (m, 29H), 2.20–2.30 (m, 2H), 2.44 (dd, J = 9.03 and 13.62 Hz, 1H), 2.87 (dd, J = 3.22 and 13.66 Hz, 1H), 3.47 (m, 1H), 3.87 (m, 1H), 5.30 (m, 1H), 7.16–7.28 (m, 5H). ^{13}C NMR δ 11.84, 19.38 (2C), 21.03, 24.24, 28.41, 31.57, 31.82 (2C), 33.91, 36.44, 37.19, 39.74, 42.21, 42.38, 43.54, 43.60, 50.01, 56.66, 56.81, 71.40, 71.72, 121.63, 126.45, 128.55 (2C), 129.42 (2C), 138.60, 140.71. Anal. calcd for ($C_{30}H_{44}O_2$): C, 82.51 %; H, 10.16 %. Found: C, 82.88 %; H, 10.25 %.

4.1.5.13. 23(R)-24-phenylchol-5-en-3β,23-diol (23). Following general procedure D **23** was obtained starting from **35** in 77 % yield as a white solid (eluent: light petroleum/EtOAc, 8:2, v/v). M.p. = 130–131 °C. ^{1}H NMR δ 0.65 (s, 3H), 0.86–2.00 (m, 29H), 2.14–2.26 (m, 2H), 2.60–2.71 (m, 2H), 3.45 (m, 1H), 3.87 (m, 1H), 5.30 (m, 1H), 7.15–7.28 (m, 5H). ^{13}C NMR δ 11.89, 18.48, 19.35, 21.02, 24.21, 28.36, 31.56, 31.81 (2C), 32.48, 36.43, 37.18, 39.77, 42.20, 42.42, 43.32, 45.22, 50.02, 56.66, 56.77, 69.74, 71.73, 121.63, 126.38, 128.50 (2C), 129.36 (2C), 138.67, 140.70. Anal. calcd for ($C_{30}H_{44}O_2$): C, 82.51 %; H, 10.16 %. Found: C, 82.90 %; H, 10.26 %.

4.1.5.14. 22(S)-3β-hydroxy-24-norchol-5-en-22-yl acetate (42a). Following general procedure D **42a** was obtained starting from **41a** in 70 % yield as an oil (eluent: light petroleum/EtOAc, 80:20, v/v). ^{1}H NMR δ 0.56 (m, 3H), 0.82–1.91 (m, 31H), 2.12–2.19 (m, 2H), 2.34 (s, 1H), 3.40 (m, 1H), 4.91 (m, 1H), 5.23 (m, 1H); ^{13}C NMR δ 11.58, 12.64, 17.75, 19.27, 20.94, 21.24, 24.09, 27.69, 31.39, 31.69, 31.78, 36.34, 37.12, 39.56, 40.54, 42.06 (2C), 49.93, 52.47, 56.41, 71.46, 72.57, 121.42, 140.66, 170.88.

4.1.5.15. 22(S)-3β-Hydroxychol-5-en-22-yl acetate (42b). Following general procedure D **42b** was obtained starting from **41b** in 71 % yield as an oil (eluent: light petroleum/EtOAc, 80:20, v/v). ^{1}H NMR δ ^{1}H NMR (400 MHz, $CDCl_3$) δ 0.60 (m, 3H), 0.70–2.00 (m, 34H), 2.15–2.19 (m, 2H), 3.42 (m, 1H), 4.81 (m, 1H), 5.26 (m, 1H); ^{13}C NMR) δ 10.34, 11.59, 12.66, 19.35, 21.02, 21.21, 24.18, 24.99, 28.07, 31.53, 31.77, 36.41, 37.18, 38.49, 39.65, 42.18 (2C), 50.00, 52.43, 56.56, 71.66, 77.66, 121.62, 140.65, 171,07.

4.1.5.16. 22(S)-3β-hydroxy-24-norcholest-5-en-22-yl acetate (42c). Following general procedure D **42c** was obtained starting from **41c** in 71 % yield as an oil (eluent: light petroleum/EtOAc, 80:20, v/v). ^{1}H NMR δ 0.60 (m, 3H), 0.83–1.95 (m, 38H), 2.15–2.20 (m, 2H), 3.45 (m, 1H), 5.00 (m, 1H), 5.27 (brs, 1H); ^{13}C NMR δ 11.60, 12.96, 19.37, 21.03, 21.27, 22.64, 22.78, 24.24, 24.76, 28.12, 31.57, 31.87 (2C), 36.43, 37.19, 39.45, 39.66, 41.28, 42.22 (2C), 50.02, 52.55, 56.53, 71.71, 74.61, 121.66, 140.64, 170.92.

4.1.5.17. 22(S)-3β-hydroxy-23-phenyl-24-norcholest-5-en-22-yl acetate (42d). Following general procedure E **42d** was obtained starting from **41d** in 59 % yield as an oil (eluent: light petroleum/EtOAc, 80:20, v/v). ^{1}H NMR δ 0.50 (m, 3H), 0.83–1.90 (m, 29H), 2.14–2.19 (m, 2H), 2.65 (dd, J = 7.2 and 13.4 Hz, 1H), 2.84 (dd, J = 7.3 and 13.4 Hz, 1H), 3.43 (m, 1H), 5.12 (t, J = 7,2 Hz, 1H), 5.26 (brs, 1H), 7.10–7.22 (m, 5H); ^{13}C NMR δ 11.47, 12.83, 19.31, 20.96, 21.09, 24.09, 27.96, 31.47, 31.70, 31.77, 36.36, 37.14, 37.97, 38.25, 39.58, 42.12 (2C), 49.94, 52.40, 56.49, 71.58, 76.87, 121.54, 126.27, 128.29 (2C), 129.15 (2C), 137.86, 140.62, 170.61.

4.1.6. General procedure E – sulfation reaction and subsequent alkaline treatment

Sulfur trioxide-pyridine complex (2 eq) was added to a stirred solution of the sterol (1 eq) in dry pyridine (6 mL/mmol) and the resulting mixture was stirred at room temperature under argon atmosphere. After 12 h cold light petroleum (6 mL/mmol) was added and the precipitate, thus formed, was separated by vacuum filtration and then washed with cold light petroleum. The solid was then suspended in 1.25 M NaOH in MeOH (6 mL/mmol) and the resulting mixture heated at reflux for 3 h. After further 12 h of stirring at room temperature, H_2O (2 mL/mmol)) was added and the resulting precipitate isolated by vacuum filtration, washed with H_2O and acetone and finally dried in vacuum.

4.1.6.1. Sodium 22(R)-22-Hydroxycholest-5-en-3β-yl sulfate (17). Following general procedure E **17** was obtained starting from **40** in 54 % yield as a white solid. M.p. 196–198 °C; ^{1}H NMR δ 0.53 (s, 3H), 0.70–1.80 (m, 37H), 1.99–2.05 (m, 1H), 2.24–2.22 (m, 1H), 3.26 (m, 1H), 3.72 (m, 1H), 5.17 (s, 1H); ^{13}C NMR (DMSO-d_6) δ 12.24, 13.01, 19.59, 21.14, 22.96, 23.54, 24.56, 27.33, 27.56, 28.09, 29.32, 32.01, 36.46, 36.61, 37.41, 42.53, 42.63, 50.10, 53.33, 56.22, 71.85, 75.80, 121.67, 141.21. Anal. calcd for ($C_{27}H_{45}NaO_5S$): C, 64.25 %; H, 8.99 %; S, 6.35 %. Found: C, 64.30 %; H, 9.02 %; S, 6.18 %.

4.1.6.2. Sodium 22(S)-22-hydroxy-24-norchol-5-en-3β-yl sulfate (19a). Following general procedure E **19a** was obtained starting from **42a** in 55 % yield as a white solid. M.p. 201–202 °C; ^{1}H NMR (DMSO-d_6) δ 0.54 (m, 3H), 0.70–1.50 (m, 23H), 1.70–1.90 (m, 5H), 2.04 (m, 1H), 2.26 (m, 1H), 3.31 (s, 1H), 3.60 (m, 1H), 3.75 (m, 1H), 5.19 (s, 1H); ^{13}C NMR (DMSO-d_6) δ 12.20 (2C), 19.60, 21.18, 22.07, 24.47, 27.77, 29.32, 32.08 (2C), 36.64, 37.41, 42.20, 42.31, 50.14, 52.73, 56.76, 67.20, 75.98, 121.73, 141.22. Anal. calcd for ($C_{23}H_{37}NaO_5S$): C, 61.58 %; H, 8.31 %; S, 7.15 %. Found: C, 61.97 %; H, 8.42 %; S, 7.00 %.

4.1.6.3. Sodium 22(S)-22-Hydroxychol-5-en-3β-yl sulfate (19b). Following general procedure E **19b** was obtained starting from **42b** in 52 % yield as a white solid. mp 228 °C (decomposition); ^{1}H NMR (DMSO-d_6) δ 0.50–2.00 (m, 34H), 2.14 (m, 1H), 2.37 (m, 1H), 3.84 (brs, 1H), 4.03 (brs, 1H), 5.28 (brs, 1H); ^{13}C NMR (DMSO-d_6) δ 11.64, 12.21, 12.29, 19.61, 21.18, 24.42, 27.85, 28.31, 29.32, 32.06, 36.64, 37.40, 42.19, 50.12, 52.50, 56.83, 73.39, 75.91, 121.70, 141.23. Anal. calcd for ($C_{24}H_{39}NaO_5S$): C, 62.31 %; H, 8.50 %; S, 6.93 %. Found: C, 62.78 %; H, 8.59 %; S, 6.88 %.

4.1.6.4. Sodium 22(S)-22-hydroxy-24-norcholest-5-en-3β-yl sulfate (19c). Following general procedure E **19c** was obtained starting from **42c** in 40 % yield as a white solid. M.p. 195 °C (decomposition); ^{1}H NMR (DMSO-d_6) δ 0.54 (s, 3H), 0.70–2.00 (m, 35H), 2.04 (m, 1H), 2.26–2.29 (m, 1H), 3.74 (m, 1H), 3.90 (m, 1H), 5.19 (s, 1H); ^{13}C NMR (DMSO-d_6) δ 12.22, 12.48, 19.63, 21.18, 23.08, 23.79, 24.44, 24.98, 27.87, 29.34, 32.06, 36.65, 37.41, 41.13, 42.20, 44.93, 50.10, 52.62, 56.81, 69.35, 75.88, 121.72, 141.24. Anal. calcd for ($C_{26}H_{43}NaO_5S$): C, 63.64 %; H, 8.83 %; S, 6.53 %. Found: C, 63.79 %; H, 8.91 %; S, 6.49 %.

4.1.6.5. Sodium 22(S)-22-hydroxy-23-phenyl-24-norchol-5-en-3β-yl sulfate (19d). Following general procedure E **19d** was obtained starting from **42d** in 40 % yield as a white solid. M.p. 193–194 °C; ^{1}H NMR (DMSO-d_6) δ 0.46 (m, 3H), 0.75–1.50 (m, 22H), 1.75–1.90 (5H), 2.03 (m, 1H), 2.26–2.28 (m, 1H), 2.56–2.61 (m, 1H), 3.73 (m, 1H), 4.18 (s, 1H), 5.18 (s, 1H), 7.07–7.18 (m, 5H); ^{13}C NMR (DMSO-d_6) δ 12.38, 12.62, 19,88, 21.41, 24.62, 28.08, 29.53, 32.27, 36.87, 37.63, 42.23, 42.45, 50.36, 52.68, 57.06, 73.75, 76.51, 122.14, 126.54, 128.95, 129.92, 141.08, 141.38. Anal. calcd for ($C_{29}H_{41}NaO_5S$): C, 66.38 %; H, 7.88 %; S, 6.11 %. Found: C, 66.67 %; H, 7.99 %; S, 6.00 %.

4.1.7. 22(R)-6β-methoxy-3α,5-cyclo-5α-cholestan-22-ol (29)

Methanesulfonyl chloride (3.47 g, 30.01 mmol) was added to a stirred solution of **28k** (0.51 g, 1.34 mmol) in dry pyridine (11 mL) kept under argon atmosphere at room temperature. After 14 h, water (30 mL) was added and the mixture was extracted with EtOAc (2 x 40 mL). The combined organic layers were washed with brine (50 mL) and dried over anhydrous Na_2SO_4. Evaporation of the solvent gave an oily crude product that was dissolved in dry DMF/DMSO (1:1, 38 mL), followed by the addition of 18-crown-6 (1.49 g, 4.11 mmol) and potassium superoxide (0.49 g, 6.83 mmol). The resulting mixture was stirred at room temperature for 24 h. Water (40 mL) was added and the mixture extracted with EtOAc (2 x 35 mL). The combined organic layers were washed with brine (40 ml) and dried over anhydrous Na_2SO_4. After the removal of the volatiles at reduced pressure, the crude oily product was purified by flash chromatography. Elution with light petroleum/EtOAc (95:5, v/v) gave **29** in 70 % yield. ^{1}H NMR δ 0.31–0.32 (m, 1H), 0.53–0.55 (m, 1H), 0.63 (s, 3H), 0.70–1.70 (m, 36H), 1.77–1.89 (m, 2H), 2.66 (s, 1H), 3.21 (s, 3H), 3.49–3.51 (m, 1H); ^{13}C NMR δ 12.19, 12.34, 13.01, 19.23, 21.40, 22.42, 22.72, 22.89, 24.20, 24.90, 27.47, 28.11, 30.44, 33.27, 34.98, 35.16, 36.06, 40.18, 42.31 (2C), 42.99, 43.29, 47.96, 53.27, 56.03, 56.49, 73.92, 82.29.

4.1.8. 22(R)-3β-hydroxycholest-5-en-22-yl acetate (40)

Acetic anhydride (0.08g, 0.83 mmol) and 4-DMAP (0.01 g, 0.10 mmol) were added to a stirred solution of **29** (0.16 g, 0.40 mmol) in CH_2Cl_2 (15 mL) and pyridine (0.06 mL) kept at room temperature. After 24 h, a solution of 3 M HCl (10 mL) was added, the organic layer was separated and washed with H_2O (15 mL), brine (10 mL) and then dried over anhydrous Na_2SO_4. After the removal of the volatiles at reduced pressure, the crude product was dissolved in 1,4-dioxane (6 mL) and water (2 mL) followed by the addition of *p*-toluenesulfonic acid monohydrate (0.01 g, 0.05 mmol). The resulting mixture was warmed to 75 °C (external temperature) and stirred for 1.5 h. The reaction was quenched by diluting with water (5 mL) and then extracted with EtOAc (2 x 8 mL). The combined organic layers were washed with brine (10 mL) and dried over anhydrous Na_2SO_4. After the removal of the volatiles at reduced pressure, the crude oily product was purified by flash chromatography. Elution with light petroleum/EtOAc (80:20, v/v), gave **40** in 58 % yield as a white solid. M.p. = 137–138 °C; ^{1}H NMR δ 0.58 (s, 3H), 0.70–1.94 (m, 30H), 2.13–2.25 (m, 2H), 3.40–3.50 (m, 1H), 4.75–4.78 (m, 1H), 5.25 (m, 1H); ^{13}C NMR δ 11.74, 12.99, 19.26, 20.93, 21.32, 22.30, 22.74, 24.21, 24.72, 26.99, 27.80, 31.47, 31.74, 35.48, 36.34, 37.11, 39.09, 39.59, 42.12, 42.53 (2C), 49.96, 52.92, 56.22, 71.60, 121.49, 140.60, 170.85.

4.1.9. 22(R)-6β-methoxy-23-phenyl-3α,5-cyclo-24-nor-5α-cholan-22-yl acetate (30)

Methanesulfonyl chloride (2.37 g, 20.67 mmol) was added to a stirred solution of **28d** (0.40 g, 0.92 mmol) in dry pyridine (7.6 mL) kept under argon atmosphere at room temperature. After 15 h water (30 mL) was added and the mixture was extracted with EtOAc (2 x 30 mL). The combined organic layers were washed with brine (20 mL) and dried over anhydrous Na_2SO_4. After the removal of the volatiles at reduced pressure the crude orange oil obtained was were dissolved in dry toluene (2.2 mL), followed by the addition of 18-crown-6 (0.060 g, 0.23 mmol) and CsOAc (0.284 g, 1.48 mmol). The resulting suspension was heated to reflux and stirred for 26 h. Water (10 mL) was added and the resulting mixture was extracted with EtOAc (2 x 25 mL). The combined organic layers were washed with brine (10 mL) and dried over anhydrous Na_2SO_4. After the removal of the volatiles at reduced pressure the crude oily product was purified by flash chromatography. Elution with light petroleum/EtOAc (90:10, v/v) gave **30** in 34 % overall yield. ^{1}H NMR δ 0.45 (dd, J = 5.12 and 7.95 Hz, 1H), 0.67 (t, J = 4.78 Hz, 1H), 0.76 (s, 3H), 0.85–2.05 (m, 29H), 2.65–2.76 (m, 2H), 2.79 (s, 1H), 3.34 (s, 3H), 5.12–5.16 (m, 1H), 7.16–7.20 (m, 3H), 7.24–7.28 (m, 2H). ^{13}C NMR δ 12.24, 13.00, 13.07, 19.23, 21.08, 21.42, 22.72, 24.20, 24.90, 27.20,

30.44, 33.29, 33.76, 34.96, 35.21, 39.11, 40.22, 43.12, 43.30, 47.95, 53.24, 56.09, 56.51, 77.32, 82.25, 126.08, 128.15 (2C), 129.00 (2C), 138.91, 170.26.

4.1.10. 22(R)-23-phenyl-24-norchol-5-en-3β,22-diol (20)

p-Toluensulfonic acid monohydrate (0.003 g, 0.02 mmol) was added to a stirred solution of **30** (0.074 g, 0.15 mmol) in 1,4-dioxane (4.8 mL) and water (1.4 mL). The resulting mixture was warmed to 75 °C (external temperature) and stirred for 2.5 h. Water (15 mL) was added and the resulting mixture was extracted with EtOAc (2 x 15 mL). The combined organic layers were washed with brine (10 mL) and dried over anhydrous Na_2SO_4. After the removal of the volatiles at reduced pressure the crude gluey product obtained was dissolved in MeOH (7.3 mL) followed by the addition of 2 M aqueous NaOH (1.6 mL). The resulting suspension was heated to reflux and stirred for 1 h. The reaction was then quenched by the addition of 1 M HCl (7 mL). The resulting aqueous layer was extracted with EtOAc (2 x 30 mL). The combined organic layers were washed with brine (10 mL) and dried over anhydrous Na_2SO_4. After the removal of the volatiles at reduced pressure the crude product was purified by mpc. Elution with light petroleum/EtOAc (7:3, v/v) gave **20** in 70 % overall yield. M.p. = 225–227 °C (with decomposition). ^{1}H NMR δ 0.75 (s, 3H), 0.98–2.05 (m, 27H), 2.21–2.29 (m, 2H), 2.42–2.48 (t, J = 11.43 Hz, 1H), 2.77 (d, J = 13.43 Hz, 1H), 3.54 (m, 1H), 3.88 (m, 1H), 5.37 (m, 1H), 7.22–7.35 (m, 5H). ^{13}C NMR δ 11.91, 12.55, 19.38, 21.07, 24.42, 27.50, 31.61, 31.92 (2C), 36.48, 36.72, 37.22, 39.77, 41.34, 42.25, 42.71, 50.10, 53.22, 56.39, 71.74, 74.67, 121.56, 126.35, 128.63 (2C), 129.28 (2C), 139.70, 140.80. Anal. calcd for ($C_{29}H_{42}O_2$): C, 82.41 %; H, 10.02 %. Found: C, 82.60 %; H, 10.45 %.

4.1.11. 6β-methoxy-23-phenyl-3α,5-cyclo-24-nor-5α-cholan-22-one (31)

Dess-Martin periodinane (0.68 g, 1.60 mmol) was added to a stirred solution of **28d** (0.29 g, 0.65 mmol) in dry dichloromethane (7 mL) kept under argon at room temperature. After 3 h the reaction was quenched by the addition of 10 % aqueous solution of $Na_2S_2O_3$ (20 mL). The aqueous layer was separated and extracted with dichloromethane (3 x 20 mL). The combined organic layers were washed with brine (20 mL) and dried over anhydrous Na_2SO_4. After the removal of the volatiles at reduced pressure, the gluey crude product was purified by flash chromatography. Elution with light petroleum/EtOAc (95:5, v/v) gave **31** in 69 % yield as a white glue· ^{1}H NMR δ 0.43 (dd, J = 5.13 and 7.89 Hz, 1H), 0.65 (t, J = 4.47 Hz, 1H), 0.80–1.93 (m, 28H), 2.66 (m, 1H), 2.77 (m, 1H), 3.32 (s, 3H), 3.70 (s, 2H), 7.17–7.33 (m, 5H). ^{13}C NMR δ 12.29, 12.93, 16.50, 19.14, 21.28, 22.55, 24.22, 24.78, 27.41, 30.30, 33.18, 34.86, 35.02, 39.91, 42.80, 43.18, 47.79, 48.53, 48.74, 51.97, 55.61, 56.39, 82.10, 126.67, 128.34 (2C), 129.48 (2C), 133.95, 211.35.

4.1.12. 6β-methoxy-3α,5-cyclo-24-nor-5α-chol-22-ene (32)

1.7 M solution of potassium *tert*-pentoxide in toluene (9.5 mL, 16.00 mmol) was slowly added via syringe to a stirred suspension of methyltriphenylphosphonium bromide (5.708 g, 16.00 mmol) in dry toluene (50 mL) kept in argon atmosphere at room temperature. The resulting dark yellow suspension was stirred for 1 h at room temperature. Then, a solution of **26** (1.40 g, 4.00 mmol) in dry toluene (15 mL) was added. Once the addition was concluded, the resulting suspension was warmed to 70 °C. As the reaction proceeds the colour of the suspension changed from dark yellow to dark orange. After 1 h the system was cooled to room temperature and the reaction was quenched by the addition of water (25 mL). The organic phase was separated, and the resulting aqueous phase was further extracted with toluene (10 mL). The combined organic layers were dried over anhydrous Na_2SO_4. After the removal of the volatiles at reduced pressure the crude product was purified by flash chromatography. Elution with light petroleum/EtOAc (98:2, v/v) gave **32** in 97 % yield as a slightly yellow oil. ^{1}H NMR δ 0.33 (dd, J = 5.12 and 7.88 Hz, 1H), 0.55 (t, J = 4.58 Hz, 1H), 0.60–2.10 (m, 29H), 2.67 (s, 1H), 3.22 (s, 3H), 4.71 (dd, J = 1.76 and 10.19 Hz, 1H), 4.80 (dd, J = 1.76 Hz and 17.07 Hz, 1H), 5.56 (ddd, J = 8.54, 10.19 and 17.07 Hz, 1H). ^{13}C NMR δ 12.38, 13.03, 19.24, 20.06, 21.44, 22.72, 24.13, 24.92, 28.44, 30.43, 33.32, 35.01, 35.24, 40.15, 41.17, 42.72, 43.34, 48.03, 55.58, 56.49 (2C), 82.34, 111.48, 145.18.

4.1.13. 6β-methoxy-3α,5-cyclo-24-nor-5α-cholan-23-ol (33)

A solution of 1 M borane THF complex in THF (12.6 mL, 12.60 mmol) was added dropwise to a stirred solution of **32** (2.880 gr, 8.40 mmol) in dry THF (24 mL) kept under argon at 0 °C (internal temperature). The resulting mixture was stirred at 0 °C for 2 h. Then 6 M NaOH (14.4 mL) and 30 % hydrogen peroxide were carefully added dropwise via syringe. (CAUTION, gas and heat may be uncontrollably generated in case of fast addition of both aqueous solutions!) After 1 h the resulting white suspension was diluted with water (20 mL) and extracted with EtOAc (3 x 20 mL). The combined organic layers were dried over anhydrous Na_2SO_4. After the removal of the volatiles at reduced pressure the crude product was purified by flash chromatography. Elution by light petroleum/EtOAc (8:2, v/v) gave **33** in 94 % yield as a colourless wax. ^{1}H NMR δ 0.33 (m, 1H), 0.55 (m, 1H), 0.60–2.0 (m, 32H), 2.67 (m, 1H), 3.22 (s, 3H), 3.42–3.60 (m, 2H). ^{13}C NMR δ 12.16, 13.02, 18.81, 19.22, 21.44, 22.70, 24.10, 24.90, 28.35, 30.40, 32.88, 33.29, 34.97, 35.20, 38.92, 40.22, 42.80, 43.31, 47.94, 56.46 (2C), 60.81, 82.36.

4.1.14. 6β-methoxy-3α,5-cyclo-24-nor-5α-cholan-23-al (27)

PCC (0.88 g, 4.08 mmol) was added to a stirred solution of **33** (0.370 g, 1.02 mmol) in dry dichloromethane (10.8 mL) kept at room temperature. After 1 h of vigorous stirring, the black mixture was filtered *in vacuo* through a Celite pad and the filtrate was dried at reduced pressure. The resulting crude product was purified by flash chromatography. Elution by light petroleum/EtOAc (93:7, v/v) affording **27** in 97 % yield as a colourless oil. ^{1}H NMR δ 0.30 (dd, J = 5.13 and 7.92 Hz, 1H), 0.52 (m, 1H), 0.60–2.10 (m, 30H), 2.32 (dd, J = 1.96 and 15.50 Hz, 1H), 2.64 (m, 1H), 3.19 (s, 3H), 9.61 (dd, J = 1.20 and 3.31 Hz, 1H). ^{13}C NMR δ 12.11, 12.96, 19.15, 19.86, 21.29, 22.58, 23.97, 24.81, 28.40, 30.33, 31.50, 33.19, 34.89, 35.05, 39.95, 42.77, 43.21, 47.77, 50.75, 55.86, 56.31, 56.43, 82.14, 203.34.

4.1.15. 23(R)- and 23(S)-23-hydroxy-23-phenyl-24-norchol-5-en-3β-yl acetates (38 and 39)

A solution of **36** + **37** (0.425 g, 0.97 mmol) in glacial acetic acid (10 mL) was heated to 75 °C (external temperature) and stirred for 2.5 h. After the removal of the volatiles at reduced pressure the crude product was submitted to mpc. Elution with light petroleum/EtOAc (80:20, v/v) gave **38** in 30 % yield as a white solid. M.p. = 196–197 °C. ^{1}H NMR δ 0.69 (s, 3H), 0.75–2.00 (m, 31H), 2.26 (m, 2H), 4.54 (m, 1H), 4.72 (m, 1H), 5.32 (m, 1H), 7.19–7.28 (m, 5H). ^{13}C NMR δ 11.88, 18.44, 19.20, 20.92, 21.31, 24.15, 27.63, 28.23, 31.70, 32.78, 36.43, 36.85, 37.97, 39.65, 42.39, 46.23, 49.84, 56.52, 56.56, 71.30, 73.87, 122.51, 125.41 (2C), 127.06, 128.26 (2C), 139.46, 145.98, 170.52. Following elution with the same solvent mixture gave **39** 46 % yield as a white solid. M.p. = 127–129 °C. ^{1}H NMR δ 0.47 (s, 3H), 0.90–1.97 (m, 31H), 2.26 (m, 2H), 4.53 (m, 1H), 4.67 (dd, J = 5.40 and 8.87 Hz, 1H), 5.29 (m, 1H), 7.20–7.30 (m, 5H). ^{13}C NMR δ 11.57, 19.16, 19.30, 20.83, 21.30, 24.05, 27.59, 28.09, 31.62, 33.27, 36.40, 36.82, 37.93, 39.52, 42.17, 44.95, 49.79, 56.46 (2C), 73.43, 73.84, 122.45, 126.25 (2C), 127.52, 128.33 (2C), 139.46, 144.44, 170.48.

4.1.16. 23(R)-23-phenyl-24-norchol-5-en-3β,23-diol (24)

Potassium carbonate (0.058 g, 0.42 mmol) was added to a stirred solution of **38** (0.13 g, 0.28 mmol) in methanol (6 ml) and THF (4 mL) kept at room temperature. After 6 h a saturated solution of ammonium chloride was added (10 mL) and the resulting solution was extracted with EtOAc (2 x 20 mL). The combined organic layers were washed with brine (10 mL) and dried over anhydrous Na_2SO_4. After the removal of the volatiles at reduced pressure the crude product was purified by flash chromatography. Elution with light petroleum/EtOAc (70:30, v/v) gave

24 in 96 % yield as a white solid. M.p. = 175–177 °C. ^{1}H NMR δ 0.69 (s, 3H), 0.80–1.45 (m, 20H), 1.50–2.20 (m, 11H), 3.46 (m, 1H), 4.74 (dd, *J* = 6.06 and 10.44 Hz, 1H), 5.29 (m, 1H), 7.18–7.29 (m, 5H). ^{13}C NMR δ 11.93, 18.49, 19.35, 21.02, 24.21, 28.33, 31.53, 31.80 (2C), 32.89, 36.43, 37.18, 39.76, 42.17, 42.46, 46.26, 50.01, 56.57, 56.71, 71.47, 71.71, 121.62, 125.49 (2C), 127.21, 128.37 (2C), 140.68, 145.94. Anal. calcd for ($C_{29}H_{42}O_2$): C, 82.41 %; H, 10.02 %. Found: C, 82.91 %; H, 10.27 %.

4.1.17. 23(S)-23-phenyl-24-norchol-5-en-3β-22-diol (25)

Potassium carbonate (0.089 g, 0.64 mmol) was added to a stirred solution of **39** (0.20 g, 0.43 mmol) in methanol (9 ml) and THF (6 mL) kept at room temperature. After 6 h a saturated solution of ammonium chloride was added (10 mL) and the resulting solution was extracted with EtOAc (2 x 20 mL). The combined organic layers were washed with brine (10 mL) and dried over anhydrous Na_2SO_4. After the removal of the volatiles at reduced pressure the crude product was purified by flash chromatography. Elution with light petroleum/EtOAc (70:30, v/v) gave **25** in 78 % yield as a white solid. M.p. = 174–175 °C. ^{1}H NMR δ 0.47 (s, 3H), 0.80–1.10 (m, 14H), 1.25–1.80 (m, 15H), 2.10–2.25 (m, 2H), 3.45 (m, 1H), 4.69 (dd, *J* = 5.61 and 8.55 Hz, 1H), 5.28 (m, 1H), 7.21–7.32 (m, 5H). ^{13}C NMR δ 11.68, 19.36 (2C), 20.98, 24.16, 28.21, 31.56, 31.77, 33.40, 36.42, 37.18, 39.67, 42.20, 42.28, 45.02, 49.99, 56.58, 56.63, 71.72, 73.62, 121.61, 126.34 (2C), 127.70, 128.49 (2C), 140.69, 144.49. Anal. calcd for ($C_{29}H_{42}O_2$): C, 82.41 %; H, 10.02 %. Found: C, 82.89 %; H, 10.26 %.

4.2. Crystal structure of compounds 22 and 25

A single crystal of compound **22** and of compound **25** were submitted to X-ray data collection on an Oxford-Diffraction Xcalibur Sapphire 3 diffractometer with a graphite monochromated Mo-Kα radiation (λ = 0.71073 Å) at 293 K. The structures were solved by direct methods implemented in SHELXS-97 program. [28] The refinements were carried out by full-matrix anisotropic least-squares on F^2 for all reflections for non-H atoms by means of the SHELXL-97 program. [29] The structure of **22** crystallizes with a ethanol molecule, while **25** with a 0.5 water molecule. Crystallographic data for these structures have been deposited with the Cambridge Crystallographic Data Centre as supplementary publication no. CCDC 2293930 (**22**) and 2293929 (**25**). Copies of the data can be obtained, free of charge, on application to CCDC, 12 Union Road, Cambridge CB2 1EZ, UK; (fax: +44 (0) 1223 336 033; or e-mail: deposit@ccdc.cam.ac.uk).

4.3. Biology

T0901317 and 22*R*–HC (**1**) were purchased from Sigma. C57BL/6 mice were purchased from Charles River (Calco, Italy). Mice were maintained in the pathogen-free facility of San Raffaele Scientific Institute. Experiments were conducted in compliance with the Institutional Animal Care and Use Committee programme (IACUC n° 656, 657 and 835) and in accordance with ARRIVE guidelines. Lewis Lung Carcinoma (LLC), B16F1 and B16F1-gp100 cell lines were maintained in DMEM complete medium (10 % FBS supplemented with penicillin, streptomycin, glutamine and Hepes). Tumor cell lines were from ATCC and were tested for mycoplasma contamination.

4.4. Cell culture and Co-transfection assays

Human embryonic Kidney 293 cells (American Type Culture Collection) were cultured in Dulbecco's Modified Eagle's medium containing 10 % of fetal bovine serum at 37 °C in humidified atmosphere of 5 % CO_2. We transiently transfected HEK293 cells ($4x10^4$ cells per well) in 48 well plate with the reporter plasmids pMH100X4-TK-luc (100 ng/well), Renilla (22 ng/well) together with 100 ng/well of pCMX-Gal4-LXR-α or pCMX-Gal4-LXR-β plasmids using X-tremeGENE 9 DNA Transfection Reagent (Roche). Six hours after transfection, we treated the cells with the appropriate compound for 24 h. We analysed luciferase activities by luciferase Dual Reporter Assay Systems (Promega) according to the manufacturer's protocol. GAL4-LXRs and TK-MHC100-luc plasmids were described in Raccosta et al. [21].

4.5. Quantitative real-time-PCR

U937 cell line was differentiated in foam macrophages with phorbol 12-myristate 13-acetate (PMA) 10 ng/ml (Sigma) for 72 h at 37 °C in 10 mm dish at the concentration of 3x106 cells in 10 ml RPMI 10 % FBS. At day 3 nuclear receptor ligands were added for 6 h. Total RNA was purified by TRIZOL (Invitrogen, Carlsbad, CA, USA). Reverse transcription was performed incubating 2 μg of total RNA 1 h at 42 °C with MLV-reverse transcriptase (Promega). Quantitative PCR was performed using Sybr Green Master Mix (Applied Biosystems) and real-time PCR (Viia 7 Real Time PCR System, Applied Biosystems). All PCR reactions were done in triplicate. The comparative Ct method was used to quantify transcripts that were normalized for human GAPDH. Primers have been reported in Raccosta et al. [21].

4.6. Proliferation in-vitro

B16F1 melanoma cells and LLC lung tumor cells were seeded on 6-well plate at 10^5 cells/well. Tumor cells were treated for 72 h with vehicle, or **18d** at 10 μM. At day 3 cells were collected and counted by trypan blue.

4.7. Treatment of tumor-bearing mice with PFM037 (16) or PFM046 (18d)

Tumor-bearing mice were treated with PFM046 (**18d**) or PFM037 (**16**) 6–7 days after tumor challenge. After 6–7 days, mice were randomly assigned to either treatment or vehicle groups. Mice were injected with 300 or 400 μg of either compound given i.p. for 5 days/week. We evaluated tumor size measuring perpendicular diameters by a calliper every 2–3 days. Data are reported as the average tumor volume ± SD.

4.8. Statistical analysis

Data are expressed as mean ± SD and were analysed for significance by ANOVA with Dunnet's, or Tukey's multiple comparison tests, or uncorrected Fisher's LSD test. The analysis was performed with Prism software.

4.9. In-vitro ADME characterization

[30] The kinetic solubility has been determined from 20 mM DMSO stock solution by direct dilution in PBS pH 7.4 with 2 h of equilibration time. After filtration, samples have been analysed in RapidFire-MS/MS and compared with a standard solution in methanol. CHI/LogD has been determined using the methodology reported in the literature [26]. Plasma protein binding was measured according to the dialysis approach, using buffer diluted plasma in the matrix compart and buffer in the matrix free compart. Hepatic intrinsic clearance (CLi) in liver microsomes has been performed in frozen liver microsomes at final concentration of 0.5 mg/mL. The regenerating system was NADPH and test item has been incubated at 0.5 μM. Sampling has been done using STAR-V from Hamilton Robotics. Samples from plasma protein binding and CLi have been analysed using UHPLC-MS/MS.

4.10. In-vivo PK characterization

Compounds where administered in not threated animals i.p. at the dose of 400 μg/mouse. Blood samples where withdrawal from tail vein

by a microsampling approach. Blood was centrifuged and plasma was freezing at −20 °C. After thawing, samples were diluted with HEPES 0.1 N and were analysed by UHPLC-MS/MS using a calibration line for quantitation. The standard solutions for the calibration line were prepared in mouse plasma in the same condition of the samples; quality controls were prepared and analysed distributed in the analytical batch. Elaboration of the PK data was performed by using Phoenyx WinNonlin 8.0 an by applying a non-compartmental analysis with a linear log trapezoidal as calculation method.

CRediT authorship contribution statement

Lorenzo Pontini: Writing – original draft, Validation, Methodology, Investigation, Conceptualization. **Tommaso Angelini:** Investigation. **Pietro Palazzoli:** Investigation. **Daniela Maggioni:** Methodology, Investigation. **Gianluca Giorgi:** Writing – original draft, Methodology, Investigation. **Laura Raccosta:** Writing – original draft, Methodology, Investigation. **Giuseppe Damiano:** Investigation. **Valerio Mammoli:** Writing – original draft, Methodology, Investigation. **Niccolò Fontana:** Methodology, Investigation. **Vincenzo Russo:** Writing – original draft, Validation, Supervision, Methodology, Funding acquisition, Conceptualization. **Maura Marinozzi:** Writing – review & editing, Writing – original draft, Validation, Supervision, Project administration, Methodology, Investigation, Funding acquisition, Conceptualization.

Declaration of competing interest

The authors declare the following financial interests/personal relationships which may be considered as potential competing interests:

Vincenzo Russo reports financial support was provided by Italian Association for Cancer Research. Maura Marinozzi, Vincenzo Russo Laura Raccosta, Lorenzo Pontini has patent LXR ANTAGONISTS pending to European application N. EP23156662.1 (Filing date February 14, 2023) – PCT application n. PCT/EP2024/053768 (Filing date February 14, 2024);. If there are other authors, they declare that they have no known competing financial interests or personal relationships that could have appeared to influence the work reported in this paper.

Acknowledgements

This work was supported by the Italian Association for Cancer Research (AIRC) (IG 19016, IG 15452 and IG 26305) to V.R.

Appendix A. Supplementary data

Supplementary data to this article can be found online at https://doi.org/10.1016/j.ejmech.2024.117136.

Data availability

Data will be made available on request.

References

[1] A.J. Brown, L.J. Sharpe, M.J. Rogers, Oxysterols: from physiological tuners to pharmacological opportunities, Br. J. Pharmacol. 178 (2021) 3089–3103, https://doi.org/10.1111/bph.15073.

[2] Bethany A. Janowsky, P.J. Willy, T. Rama Devi, J.R. Falck, D.J. Mangelsdorf, An oxysterol signalling pathway mediated by the nuclear receptor LXR, Nature 383 (1996) 728–731, https://doi.org/10.1038/383728a0.

[3] J.M. Lehmann, S.A. Kliewer, L.B. Moore, T.A. Smith-Oliver, B.B. Oliver, J.-L. Su, S. S. Sundseth, D.A. Winegar, D.E. Blanchard, T.A. Spencer, T.M. Willson, Activation of the nuclear receptor LXR by oxysterols defines a new hormone response pathway, J. Biol. Chem. 272 (1997) 3137–3140, https://doi.org/10.1074/jbc.272.6.3137.

[4] B.M. Forman, B. Ruan, J. Chen, G.J. Schroepfer, R.M. Evans, The orphan nuclear receptor LXRa is positively and negatively regulated by distinct products of mevalonate metabolism, Proc. Natl. Acad. Sci. U. S. A. 94 (1997) 10588–10593, https://doi.org/10.1073/pnas.94.20.10588.

[5] L.D. Sanchez, L. Pontini, M. Marinozzi, L.C. Sanchez-Aranguren, A. Reis, I.H. K. Dias, Cholesterol and oxysterol sulfates: pathophysiological roles and analytical challenges, Br. J. Pharmacol. 178 (2021) 3327–3341, https://doi.org/10.1111/bph.15227.

[6] C. Song, R.A. Hiipakka, S. Liao, Auto-oxidized cholesterol sulfates are antagonistic ligands of liver X receptors: implications for the development and treatment of atherosclerosis, Steroids 66 (2001) 473–479, https://doi.org/10.1016/s0039-128x(00)00239-7.

[7] S. Ren, X. Li, D. Rodriguez-Agudo, G. Gil, P. Hylemon, W.M. Pandak, 25HC3S Sulfated Oxysterol, Is a potent regulator of lipid metabolism in human hepatocytes, Biochem. Biophys. Res. Commun. 360 (2007) 802–808, https://doi.org/10.1016/j.bbrc.2007.06.143.

[8] L. Xu, J.K. Kim, Q. Bai, X. Zhang, G. Kakiyama, H.-K. Min, A.J. Sanyal, W. M. Pandak, S. Ren, 5-Cholesten-3β,25-Diol 3-sulfate decreases lipid accumulation in diet-induced nonalcoholic fatty liver disease mouse model, Mol. Pharmacol. 83 (2013) 648–658, https://doi.org/10.1124/mol.112.081505.

[9] Q. Bai, X. Zhang, L. Xu, G. Kakiyama, D. Heuman, A. Sanyal, W.M. Pandak, L. Yin, W. Xie, S. Ren, Oxysterol sulfation by cytosolic sulfotransferase suppresses liver X receptor/sterol regulatory element binding protein-1c signaling pathway and reduces serum and hepatic lipids in mouse models of nonalcoholic fatty liver disease, Metabolism 61 (2012) 836–845, https://doi.org/10.1016/j.metabol.2011.11.014.

[10] T. Hassanein, C.J. McClain, V. Vatsalya, L.L. Stein, S.L. Flamm, P. Martin, M. C. Cave, M. Mitchell, B. Barton, L. Nagy, G. Szabo, A. McCullough, S. Dasarathy, J. Shah, C. Blevins, D. Scott, W. Krebs, J.E. Brown, W. Lin, Safety, pharmacokinetics, and efficacy signals of larsucosterol (DUR-928) in alcohol-associated hepatitis, Am. J. Gastroenterol. 119 (2024) 107–115, https://doi.org/10.14309/ajg.0000000000002275.

[11] Durect.com. https://www.durect.com/resource_category/larsucosterol-dur-928. (Accessed 23 February 2024).

[12] L. Xu, S. Shen, Y. Ma, J.K. Kim, D. Rodriguez-Agudo, D.M. Heuman, P.B. Hylemon, W.M. Pandak, S. Ren, 25-Hydroxycholesterol-3-Sulfate attenuates inflammatory response via PPARγ signaling in human THP-1 macrophages, Am. J. Physiol. Endocrinol. Metab. 302 (2012) E788–E799, https://doi.org/10.1152/ajpendo.00337.2011.

[13] L. Xu, Q. Bai, D. Rodriguez-Agudo, P.B. Hylemon, D.M. Heuman, W.M. Pandak, S. Ren, Regulation of hepatocyte lipid metabolism and inflammatory response by 25-hydroxycholesterol and 25-hydroxycholesterol-3-sulfate, Lipids 45 (2010) 821–832, https://doi.org/10.1007/s11745-010-3451-y.

[14] I.T. Cook, Z. Duniec-Dmuchowski, T.A. Kocarek, M. Runge-Morris, C.N. Falany, 24-Hydroxycholesterol sulfation by human cytosolic sulfotransferases: formation of monosulfates and disulfates, molecular modeling, sulfatase sensitivity, and inhibition of liver X receptor activation, Drug Metab. Dispos. 37 (2009) 2069–2078, https://doi.org/10.1124/dmd.108.025759.

[15] B.A. Janowski, M.J. Grogan, S.A. Jones, G.B. Wisely, S.A. Kliewer, E.J. Corey, D. J. Mangelsdorf, Structural requirements of ligands for the oxysterol liver X receptors LXRa and LXRβ, Proc. Natl. Acad. Sci. U.S.A. 96 (1999) 266–271, https://doi.org/10.1073/pnas.96.1.266.

[16] T.A. Spencer, D. Li, J.S. Russel, J.L. Collins, R.K. Bledsoe, T.G. Consler, L.B. Moore, C.M. Galardi, D.D. McKee, J.T. Moore, M.A. Watson, D.J. Parks, M.H. Lambert, T. M. Willson, Pharmacophore analysis of the nuclear oxysterol receptor LXRα, J. Med. Chem. 44 (2001) 886–897, https://doi.org/10.1021/jm0004749.

[17] E. Tranheim Kase, B. Andersen, H.I. Nebb, A.C. Rustan, G. Hege Thoresen, 22-Hydroxycholesterols regulate lipid metabolism differently than T0901317 in human myotubes, Biochim. Biophys. Acta - Mol. Cell Biol. Lipids 1761 (2006) 1515–1522, https://doi.org/10.1016/j.bbalip.2006.09.010.

[18] E.T. Kase, G.H. Thoresen, S. Westerlund, K. Højlund, A.C. Rustan, M. Gaster, Liver X receptor antagonist reduces lipid formation and increases glucose metabolism in myotubes from lean, obese and Type 2 diabetic individuals, Diabetologia 50 (2007) 2171–2180, https://doi.org/10.1007/s00125-007-0760-7.

[19] M. Marinozzi, F.F. Castro Navas, D. Maggioni, E. Carosati, G. Bocci, M. Carloncelli, G. Giorgi, G. Cruciani, R. Fontana, V. Russo, Side-chain modified ergosterol and stigmasterol derivatives as liver X receptor agonists, J. Med. Chem. 60 (2017) 6548–6562, https://doi.org/10.1021/acs.jmedchem.7b00091.

[20] L. Pontini, M. Marinozzi, Shedding light on the roles of liver X receptors in cancer by using chemical probes, Br. J. Pharmacol. 178 (2021) 3261–3276, https://doi.org/10.1111/bph.15200.

[21] L. Raccosta, M. Marinozzi, S. Costantini, D. Maggioni, L.M. Ferreira, G. Corna, P. Zordan, A. Sorice, D. Farinello, S. Bianchessi, M. Riba, D. Lazarevic, P. Provero, M. Mack, A. Bondanza, I. Nalvarte, J.A. Gustafsson, V. Ranzani, F. De Sanctis, S. Ugel, S. Baron, J.M.A. Lobaccaro, L. Pontini, M. Pacciarini, C. Traversari, M. Pagani, V. Bronte, G. Sitia, P. Antonson, A. Brendolan, A. Budillon, V. Russo, Harnessing the reverse cholesterol transport pathway to favor differentiation of monocyte-derived APCs and antitumor responses, Cell Death Dis. 14 (2023) 129, https://doi.org/10.1038/s41419-023-05620-7.

[22] L. Pontini, M. Marinozzi, Novel synthetic access to 24a-Homochol-5-en-24a-oate scaffold from stigmasterol, Org. Prep. Proced. Int. 53 (2021) 571–577, https://doi.org/10.1080/00304948.2021.1974260.

[23] D.J. Cram, F.A.A. Elhafez, Studies in stereochemistry. X. The rule of "steric control of asymmetric induction" in the synthesis of acyclic systems, J. Am. Chem. Soc. 74 (1952) 5828–5835, https://doi.org/10.1021/ja01143a007.

[24] N. Theobald, R.J. Wells, C. Djerassi, Minor and trace sterols in marine invertebrates. 8.1 isolation, structure elucidation, and partial synthesis of two novel sterols—stelliferasterol and isostelliferasterol, J. Am. Chem. Soc. 100 (1978) 7677–7684, https://doi.org/10.1021/ja00492a041.

[25] J.P. Dusza, J.P. Joseph, S. Bernstein, The preparation of estradiol-17β sulfates with triethylamine-sulfur trioxide, Steroids 45 (1985) 303–315, https://doi.org/10.1016/0039-128x(85)90079-0.
[26] K. Valkó, C. Bevan, D. Reynolds, Chromatographic hydrophobicity index by fast-gradient RP-HPLC: a high-throughput alternative to log P/log D, Anal. Chem. 69 (1997) 2022–2029, https://doi.org/10.1021/ac961242d.
[27] W.G. Kofron, L.M. Baclawski, A convenient method for estimation of alkyllithium concentrations, J. Org. Chem. 41 (1976) 1879–1880, https://doi.org/10.1016/S0022-328X(00)89863-0.
[28] G.M.A. Sheldrick, Short history of SHELXtle, Acta Crystallogr. A 64 (2008) 112–122, https://doi.org/10.1107/s0108767307043930.
[29] G.M. Sheldrick, Crystal structure refinement with SHELXL, Acta Crystallogr. C, Struct. Chem. 71 (2015) 3–8, https://doi.org/10.1107/s2053229614024218.
[30] M.B. Morelli, C. Amantini, M. Nabissi, G. Santoni, B. Wünsch, D. Schepmann, C. Cimarelli, M. Pellei, C. Santini, S. Fontana, V. Mammoli, W. Quaglia, A. Bonifazi, M. Giannella, G. Giorgioni, A. Piergentili, F. Del Bello, Role of the NMDA receptor in the antitumor activity of chiral 1,4-dioxane ligands in MCF-7 and SKBR3 breast cancer cells, ACS Med. Chem. Lett. 10 (2019) 511–516, https://doi.org/10.1021/acsmedchemlett.8b00536.